NASA TECHNICAL NOTE

NASA TN D-7349

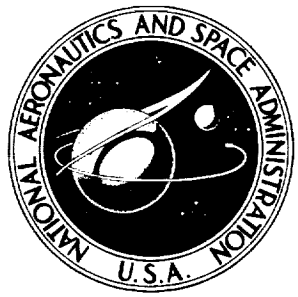

NASA TN D-7349

COMPENSATION BASED ON LINEARIZED ANALYSIS FOR A SIX-DEGREE-OF-FREEDOM MOTION SIMULATOR

by Russell V. Parrish, James E. Dieudonne, Dennis J. Martin, Jr., and James L. Copeland

Langley Research Center
Hampton, Va. 23665

NATIONAL AERONAUTICS AND SPACE ADMINISTRATION • WASHINGTON, D. C. • NOVEMBER 1973

1. Report No. NASA TN D-7349	2. Government Accession No.	3. Recipient's Catalog No.
4. Title and Subtitle COMPENSATION BASED ON LINEARIZED ANALYSIS FOR A SIX-DEGREE-OF-FREEDOM MOTION SIMULATOR		5. Report Date November 1973 6. Performing Organization Code
7. Author(s) Russell V. Parrish, James E. Dieudonne, Dennis J. Martin, Jr., and James L. Copeland		8. Performing Organization Report No. L-9023 10. Work Unit No. 501-39-11-02
9. Performing Organization Name and Address NASA Langley Research Center Hampton, Va. 23665		11. Contract or Grant No. 13. Type of Report and Period Covered Technical Note
12. Sponsoring Agency Name and Address National Aeronautics and Space Administration Washington, D.C. 20546		14. Sponsoring Agency Code

15. Supplementary Notes

Dennis J. Martin, Jr., is an employee of Electronic Associates, Inc.

16. Abstract

The inertial response characteristics of a synergistic, six-degree-of-freedom motion base are presented in terms of amplitude ratio and phase lag as functions of frequency data for the frequency range of interest (0 to 2 Hz) in real-time, digital, flight simulators. The notch filters which smooth the digital-drive signals to continuous-drive signals are presented, and appropriate compensation, based on the inertial response data, is suggested. The existence of an inverse transformation that converts actuator extensions into inertial positions makes it possible to gather the response data in the inertial axis system.

17. Key Words (Suggested by Author(s))	18. Distribution Statement
Linear compensation Motion base response Synergistic motion simulators Motion simulators	Unclassified – Unlimited

19. Security Classif. (of this report)	20. Security Classif. (of this page)	21. No. of Pages	22. Price*
Unclassified	Unclassified	36	Domestic, $3.00 Foreign, $5.50

*For sale by the National Technical Information Service, Springfield, Virginia 22151

COMPENSATION BASED ON LINEARIZED ANALYSIS FOR A SIX-DEGREE-OF-FREEDOM MOTION SIMULATOR

By Russell V. Parrish, James E. Dieudonne, Dennis J. Martin, Jr.,*
and James L. Copeland
Langley Research Center

SUMMARY

The inertial response characteristics of a synergistic, six-degree-of-freedom motion base are presented in terms of amplitude ratio and phase lag as functions of frequency data for the frequency range of interest (0 to 2 Hz) in real-time, digital, flight simulators. The notch filters which smooth the digital-drive signals to continuous-drive signals are presented, and appropriate compensation, based on the inertial response data, is suggested. The existence of an inverse transformation that converts actuator extensions into inertial positions makes it possible to gather the response data in the inertial axis system.

INTRODUCTION

Since the capabiltiy of supplying motion cues to the pilot of a flight simulator is highly desirable for certain flight tasks, the acquisition of a six-degree-of-freedom motion base (with a payload weight of about 44 480 N (10 000 lb)) has added a new dimension to flight simulation at Langley Research Center. Reference 1 documents some of the computer software necessary to produce the motion cue commands (motion base inertial position) from the aircraft equations of motion. This particular base, being synergistic in nature, does not have independent drive systems for each degree of freedom, but achieves motion in all degrees of freedom by a combination of six actuator extensions. The transformation which converts the commanded inertial position of the base into a set of actuator extensions and a method for computing the inverse transformation are documented in reference 2.

Before a motion base can be incorporated into a flight simulator, it is necessary to investigate thoroughly the response characteristics of the base, since these characteristics determine preferable operating ranges as well as suggest areas for possible compensation. This paper documents these characteristics in terms of amplitude and phase for the frequency range of interest (0 to 2 Hz), introduces the notch filter characteristics necessary for smoothing the digital drive commands into continuous drive signals, and also describes

*Electronic Associates, Inc.

appropriate compensation determined from the response characteristics. It should be noted that the purposes of this report did not include determining that the hardware met its dynamic specifications, a conclusion that was made during the acceptance test on the motion hardware system.

As emphasized in reference 2, the synergistic design requires that the control of the base be supplied through a transformation of the command inertial position into a set of actuator extensions. The nonlinear nature of the synergistic design, which is reflected in this transformation, and the characteristics of the servo drive systems result in nonlinear inertial response characteristics of the motion base. However, linear analysis methods were used to examine the response characteristics of the base, in terms of amplitude ratio and phase lag as functions of frequency of steady-state sinusoidal inputs. It should be pointed out that the existence of a real-time inverse transformation (ref. 2) makes it possible to gather the response data in terms of inertial position. Without this inverse transformation, the position response data would have to be in terms of actuator extensions. This fact is important in that compensation for hardware lag is readily available in the inertial washout software. (Velocity and acceleration terms already exist; see ref. 1.)

The use of linear methods for the analysis of nonlinear response characteristics is often inconclusive, but a major emphasis of this paper is to demonstrate by the consistency of the results from several types of response-generation techniques that the dynamics of the hardware is sufficiently linear to be examined by these techniques. The types of response-generation techniques used are the standard constant-amplitude frequency sweep and a peak-constant-velocity frequency sweep.

The response data available from the linear analysis is then studied in order to determine the appropriate lead which will compensate for the phase lag of the motion base. The compensation is applied to each of the degrees of freedom of the motion base, and the resulting compensated response characteristics are presented.

SYMBOLS

Measurements and calculations were made in U.S. Customary Units. They are presented herein in the International system of units (SI) with the equivalent values given parenthetically in U.S. Customary Units.

A_i translational channel lead parameters, sec^2

B_i translational channel lead parameters, sec

g gravitational constant, m/sec^2 $(in./sec^2)$

$K_{\psi L}, K_{\theta L}, K_{\phi L}$ rotational channel lead parameters, sec

ℓ_i actuator extension command previous to notch filtering, m (in.)

ℓ_o actuator extension command after notch filtering, m (in.)

P_b actual base position for a single degree of freedom, m (in.) or deg

$P_{b,max}$ maximum base position for a single degree of freedom achieved during a steady-state cycle, m (in.) or deg

$P_{I,max}$ maximum amplitude of sinusoidal drive signal, m (in.) or deg

s Laplace operator

x,y,z translational degrees of freedom in base inertial axis system, m (in.)

ζ_1, ζ_2 damping parameters of notch filters

Φ_b angle corresponding to point P_b on drive signal sine wave, deg

ψ, θ, ϕ rotational degrees of freedom in base inertial axis system, deg

ω_1, ω_2 frequency parameters of notch filters

A dot over a symbol indicates time derivative of that variable. A caret (^) over a symbol indicates a compensated variable.

PROCEDURE

The real-time system (RTS) of the digital computer complex at Langley Research Center was used to obtain the amplitude and phase response data. Figure 1 depicts a block diagram of the data collecting circuit. The drive program generates the input signals used to drive each inertial degree of freedom. These signals are sinusoidal with constant amplitude and frequency. The drive program is implemented on the RTS so that the operator can select the desired amplitude, frequency, and degree of freedom to be driven.

The actuator extension transformation (ref. 2) converts the inertial commands (x,y,z,ψ,θ,ϕ) into a set of actuator extensions, which are then provided to the hardware

through digital-to-analog converters (DAC) every 1/32 second. In order to provide the continuous signals necessary to drive the motion base, six identical notch filters, one per actuator, have been added to the hardware. These notch filters remove the 32-Hz stair-stepping effect of the DAC and replace the second-order low-pass filters that were delivered with the hardware, since the cut-off frequency of the low-pass filters was below the frequency range of interest in flight simulation. Figure 2 presents the transfer function and a circuit diagram of the notch filter, and figure 3 presents a plot of amplitude and phase characteristics as functions of frequency.

The hardware provides six signals which correspond to the actual actuator extensions achieved by the motion base. These signals, after analog-to-digital (ADC) conversion, are used to estimate the base position actually achieved, through the inverse transformation described in reference 2. Time histories of drive position are compared with the time histories of actual base position in order to calculate the amplitude-ratio and phase-lag characteristics of the base.

The amplitude ratio A_{out}/A_{in} for each degree of freedom is obtained by dividing the peak amplitude of the actual base positions $P_{b,max}$ by the peak amplitude of the drive signal $\left(\text{sine wave of amplitude } P_{I,max}\right)$. Ratios are calculated for both the positive and negative peak positions. To obtain the phase lag, one cycle of the drive signal is compared with the base position time history during a steady-state cycle. (See fig. 4.) Since the phase lag of the base is not constant, it is determined for the following four points:

(1) Drive signal position = 0, drive signal velocity < 0

(2) Drive signal position is at the negative peak, drive signal velocity = 0

(3) Drive signal position = 0, drive signal velocity > 0

(4) Drive signal position is at the positive peak, drive signal velocity = 0

At each of these four points actual base position P_b in a particular degree of freedom is related to a corresponding point on the drive signal sine wave. The angle Φ_b corresponding to this point is calculated as

$$\Phi_b = \arcsin \frac{P_b}{|P_{b,max}|}$$

The phase lag of the base is then defined as the difference between the drive angle (0^o, 90^o, 0^o, and -90^o for the four points, respectively) and Φ_b. The maximum phase lag obtained from the four points is then used as the phase lag presented in the data.

Figure 4 presents a time-history comparison of drive signal and actual base position for an input amplitude of 0.0203 m (0.8 in.) and a frequency of 2.5 rad/sec. This case is

presented to illustrate the nonlinear response characteristics of the base, particularly evident in low-peak-velocity cases. Note the differences for positive and negative peaks as well as the phase differences at the four phase data points.

RESPONSE CHARACTERISTICS

Since the six-degree-of-freedom base is a position command system, all the data on response characteristics presented will be position data. Although the hardware is capable of exceeding the manufacturer's specified velocity and acceleration limits (shown in table I for single-degree-of-freedom operation) at certain points in the operating region, it is recommended that these limits be accepted for operation in a flight simulator, inasmuch as the limits are representative of the minimum of the true limits under multi-degree-of-freedom operation. Thus, most of the data presented will be within the position, velocity, and acceleration limits. It should be mentioned that the hardware servo parameters were set to values which yielded a subjectively smooth ride, but did not necessarily give the best possible response.

Constant-Amplitude Response

Figure 5 presents the amplitude and phase response of the motion base for a constant-amplitude sinusoidal input of 0.0457 m (1.8 in.) in the translational degrees of freedom. Figure 6 presents similar data for an input amplitude of 1.2^{o} in the rotational degrees of freedom. The data are presented only over the range of frequency that would likely be encountered in a real-time digital simulation (around 1 to 2 Hz maximum). The amplitude ratios are presented for both the positive and negative peaks, whereas the phase data present the maximum phase lag encountered over a steady-state cycle.

It should be mentioned that the data are repeatable on a day-to-day basis, and also on a neutral-point-to-neutral-point basis. (The neutral point is defined as the selected position of the base when all degrees of freedom are at zero position.) However, it was discovered that the response of the base varied somewhat with the magnitude of amplitude. For example, the amplitude and phase data would be slightly different for a constant-amplitude sinusoidal input of 0.1524 m (6 in.) as compared with the data for 0.0457 m (1.8 in.). Thus, an obvious nonlinear characteristic suggested further investigation. The data for amplitudes of 0.0457 m (1.8 in.) and 1.2^{o} are presented since the excitation invoked over the range of frequencies is within the velocity and acceleration limits.

Constant-Peak-Velocity Response

After the base response was found to be amplitude dependent, an attempt was made to evaluate the effect of this dependence on the assumption of sufficient linearity. Addi-

tional data were collected to determine the base response to several constant-peak-velocity sinusoidal inputs over the frequency range and, when possible, within the accepted operational limits of table I. As the frequency of the drive signal was increased, the amplitude was decreased to maintain a constant peak velocity. Three peak velocity cases were considered for each of the translational degrees of freedom, and three similar cases were considered for each of the rotational degrees of freedom.

The three peak velocity cases for the translational degrees of freedom were

(1) High velocity or 0.508 m/sec (20 in./sec)

(2) Medium velocity or 0.254 m/sec (10 in./sec)

(3) Low velocity or 0.0508 m/sec (2 in./sec)

The values of the drive amplitude and frequency, and the resulting commanded accelerations, are shown in table II. The results of this investigation are presented in figure 7. A comparison of the data of figure 7 with the data of figure 5 lends confidence to the linearity assumption, with the exception of the low-peak-velocity case. However, since the magnitudes of the acceleration imparted during this case are so low (near the subliminal level), it is felt that the effect on flight simulation would be slight.

The three peak-velocity cases for the rotational degrees of freedom were

(1) High velocity or 14^{o}/sec

(2) Medium velocity or 7^{o}/sec

(3) Low velocity or 1^{o}/sec

Figure 8 presents similar data for the rotational channels (the values of amplitude, frequency, and commanded acceleration are shown in table III), and a comparison with figure 6 leads to the same conclusions as those obtained for the translational channels.

COMPENSATION

An analysis of the data revealed that the hardware had dominant second-order phase lag characteristics (ref. 3, ch. 6). Compensation for these lags should be achieved by the introduction of appropriate second-order lead circuits to the motion software package. (See ref. 1 and compensation block in fig. 1.) These lead circuits require as inputs both the first and second derivatives of the signal to be compensated. However, the design of the washout portion of the software only provides the required derivatives for the translational degrees of freedom. In the rotational degrees of freedom, only the first derivatives of the drive signals are available; thus the compensation is limited to first order.

Compensation for the Translational Degrees of Freedom

The second-order compensation for the three translational degrees of freedom is of the form

$$\hat{x} = x + B_1\dot{x} + A_1\ddot{x}$$

$$\hat{y} = y + B_2\dot{y} + A_2\ddot{y}$$

$$\hat{z} = z + B_3\dot{z} + A_3\ddot{z}$$

The values of the compensation parameters are presented in table IV whereas the compensated response data are presented in figure 9 for the constant-amplitude case. Note that the phase lag was reduced from a peak of about 85° at 2 Hz to a near constant lag of about 11°.

Compensation for the Rotational Degrees of Freedom

The first-order compensation for lag in the rotational degrees of freedom is of the form

$$\hat{\psi} = \psi + K_{\psi,L}\dot{\psi}$$

$$\hat{\theta} = \theta + K_{\theta,L}\dot{\theta}$$

$$\hat{\phi} = \phi + K_{\phi,L}\dot{\phi}$$

Again, the compensation parameters are presented in table IV, and the compensated response data for the rotational channels are presented in figure 10 for the constant-amplitude case. The reduction in phase lag was from a peak of about 130° at 2 Hz to a near constant lag of about 10°.

CONCLUDING REMARKS

The response characteristics of a synergistic six-degree-of-freedom motion base have been identified by using two types of response-generation techniques: the standard constant-amplitude frequency sweep and a peak-constant-velocity frequency sweep. The data obtained from these linear analyses suggested compensation, which, when applied to the base, reduced the phase lag from a peak of about 85° at 2 Hz in the translational

degrees of freedom to a constant lag of about 11^{o} throughout the range of 0 to 2 Hz. In the rotational degrees of freedom, the lag was reduced from a peak of about 130^{o} at 2 Hz to a constant lag of about 10^{o} throughout the range of 0 to 2 Hz. The notch filters required to remove the 32-Hz stair-stepping effect of the digital-to-analog converters have been designed, built, and integrated into the motion system.

Langley Research Center,
National Aeronautics and Space Administration,
Hampton, Va., September 4, 1973.

REFERENCES

1. Parrish, Russell V.; Dieudonne, James E.; and Martin, Dennis J.: Motion Software for a Synergistic Six-Degree-of-Freedom Motion Base. NASA TN D-7350, 1973.

2. Dieudonne, James E.; Parrish, Russell V.; and Bardusch, Richard E.: An Actuator Extension Transformation for a Motion Simulator and an Inverse Transformation Applying Newton-Raphson's Method. NASA TN D-7067, 1972.

3. Thaler, George J.; and Brown, Robert G.: Analysis and Design of Feedback Control Systems. Second ed., McGraw-Hill Book Co., Inc., c.1960.

TABLE I.- PERFORMANCE LIMITS FOR SINGLE-DEGREE-OF-FREEDOM OPERATION WITH A NEUTRAL POINT OF 0.6161 m

Degrees of freedom	Performance limits		
	Position	Velocity	Acceleration
Longitudinal, x	Forward 1.245 m Aft 1.219 m	±0.610 m/sec	±0.6g
Lateral, y	Left 1.219 m Right 1.219 m	±0.610 m/sec	±0.6g
Vertical, z	Up 0.991 m Down 0.762 m	±0.610 m/sec	±0.8g
Yaw, ψ	±32°	±15°/sec	±50°/sec^2
Pitch, θ	+30° -20°	±15°/sec	±50°/sec^2
Roll, ϕ	±22°	±15°/sec	±50°/sec^2

TABLE II.- AMPLITUDE AND ACCELERATION DATA FOR THE PEAK-VELOCITY CASES

[High velocity, 0.50813 m/sec; medium velocity, 0.25407 m/sec; low velocity, 0.05081 m/sec; translational degrees of freedom]

Frequency, rad/sec	Amplitude, m	Acceleration, g	Amplitude, m	Acceleration, g	Amplitude, m	Acceleration, g
	High velocity		Medium velocity		Low velocity	
0.10	Amplitude limits		Amplitude limits		0.50813	0.00052
.15					.33875	.00078
.25					.20325	.00130
.40			0.63516	0.01036	.12703	.00207
.70	0.72590	0.03627	.36295	.01813	.07259	.00363
1.00	.50813	.05181	.25407	.02590	.05081	.00518
1.50	.33875	.07771	.16938	.03886	.03388	.00777
2.50	.20325	.12952	.10163	.06476	.02033	.01295
4.00	.12703	.20723	.06352	.10362	.01270	.02072
6.28	.08087	.32552	.04044	.16276	.00809	.03255
9.00	.05646	.46627	.02823	.23314	.00565	.04663
12.57	.04044	*.65104	.02022	.32552	.00404	.06510

*Exceeds manufacturer's prescribed performance limits.

TABLE III.- AMPLITUDE AND ACCELERATION DATA FOR THE PEAK-VELOCITY CASES

[High velocity, 14.000 deg/sec; medium velocity, 7.000 deg/sec; low velocity, 1.000 deg/sec; rotational degrees of freedom]

Frequency, rad/sec	Amplitude, deg	Acceleration, deg/sec^2	Amplitude, deg	Acceleration, deg/sec^2	Amplitude, deg	Acceleration, deg/sec^2
	High velocity		Medium velocity		Low velocity	
0.100					10.000	0.100
.150	Amplitude limits		Amplitude limits		6.667	.150
.250					4.000	.250
.400			17.500	2.800	2.500	.400
.700	20.000	9.800	10.000	4.900	1.429	.700
1.000	14.000	14.000	7.000	7.000	1.000	1.000
1.500	9.333	21.000	4.667	10.500	.667	1.500
2.500	5.600	35.000	2.800	17.500	.400	2.500
4.000	3.500	*56.000	1.750	28.000	.250	4.000
6.283	2.228	*87.965	1.114	43.982	.159	6.283
9.000	Acceleration limits		.777	*63.000	.111	9.000
12.567			.557	*87.965	.076	12.567

*Exceeds manufacturer's prescribed performance limits.

TABLE IV.- COMPENSATION PARAMETERS

Degrees of freedom	Velocity term	Acceleration term
x	$B_1 = 0.15$	$A_1 = 0.007$
y	$B_2 = 0.15$	$A_2 = 0.007$
z	$B_3 = 0.1333$	$A_3 = 0.007$
ψ	$K_{\psi L} = 0.15$	
θ	$K_{\theta L} = 0.15$	
ϕ	$K_{\phi L} = 0.15$	

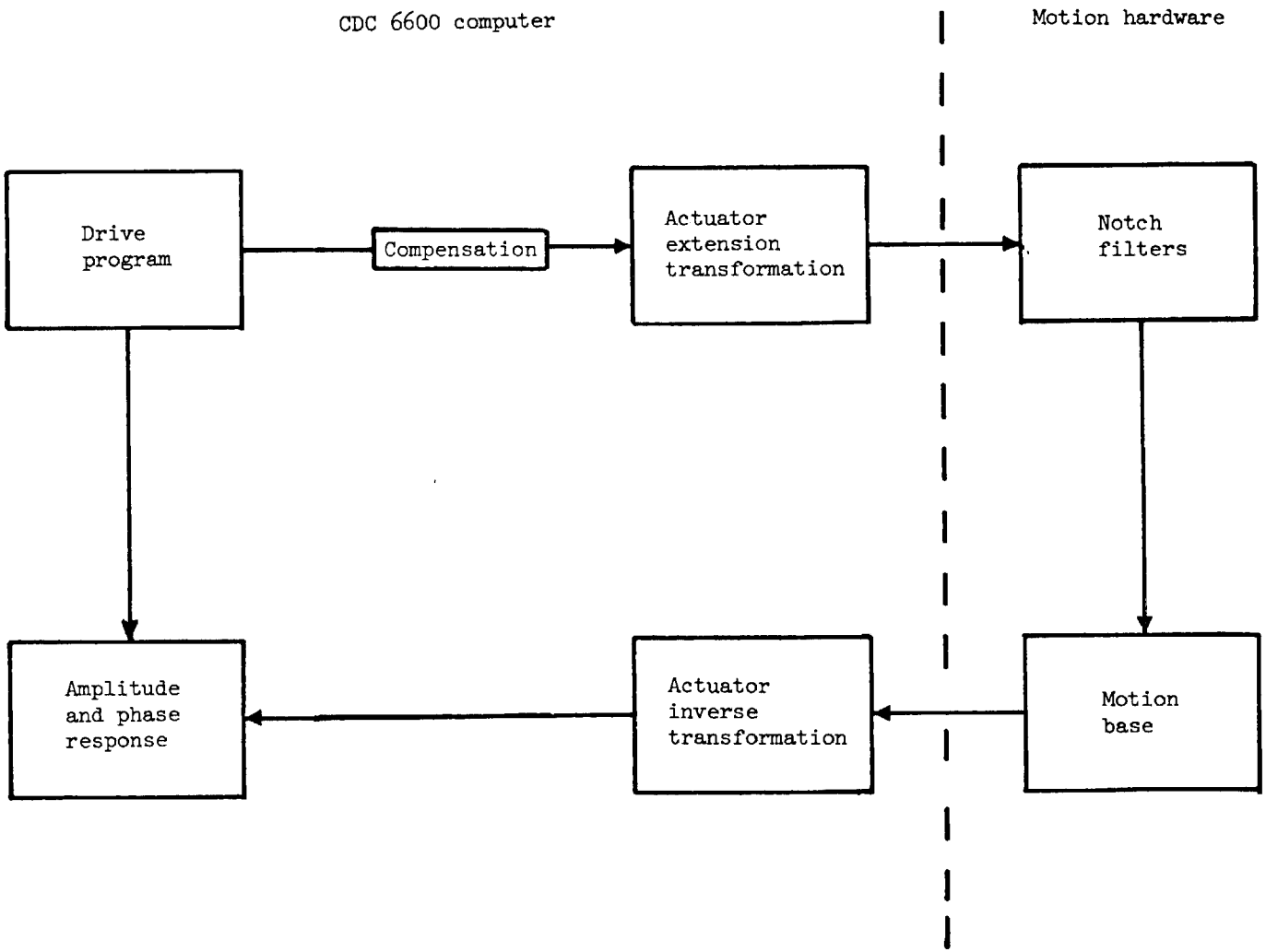

Figure 1.- Block diagram of data-collecting circuit.

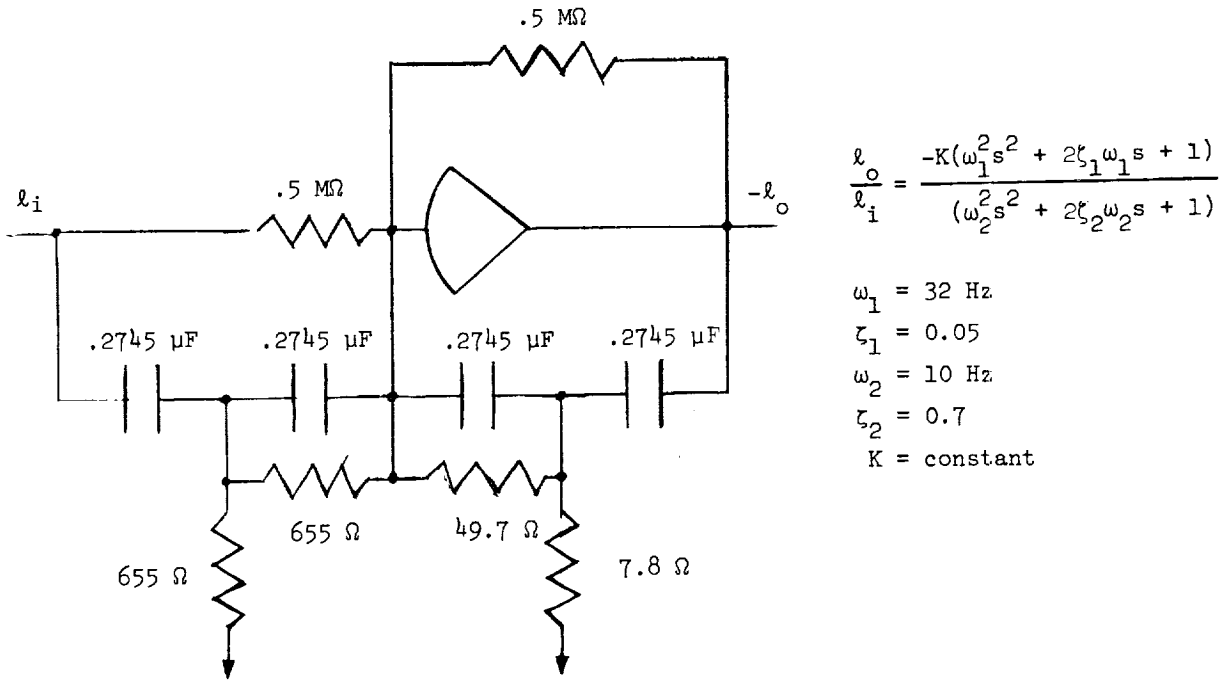

Figure 2.- Circuit diagram and transfer function of notch filter.

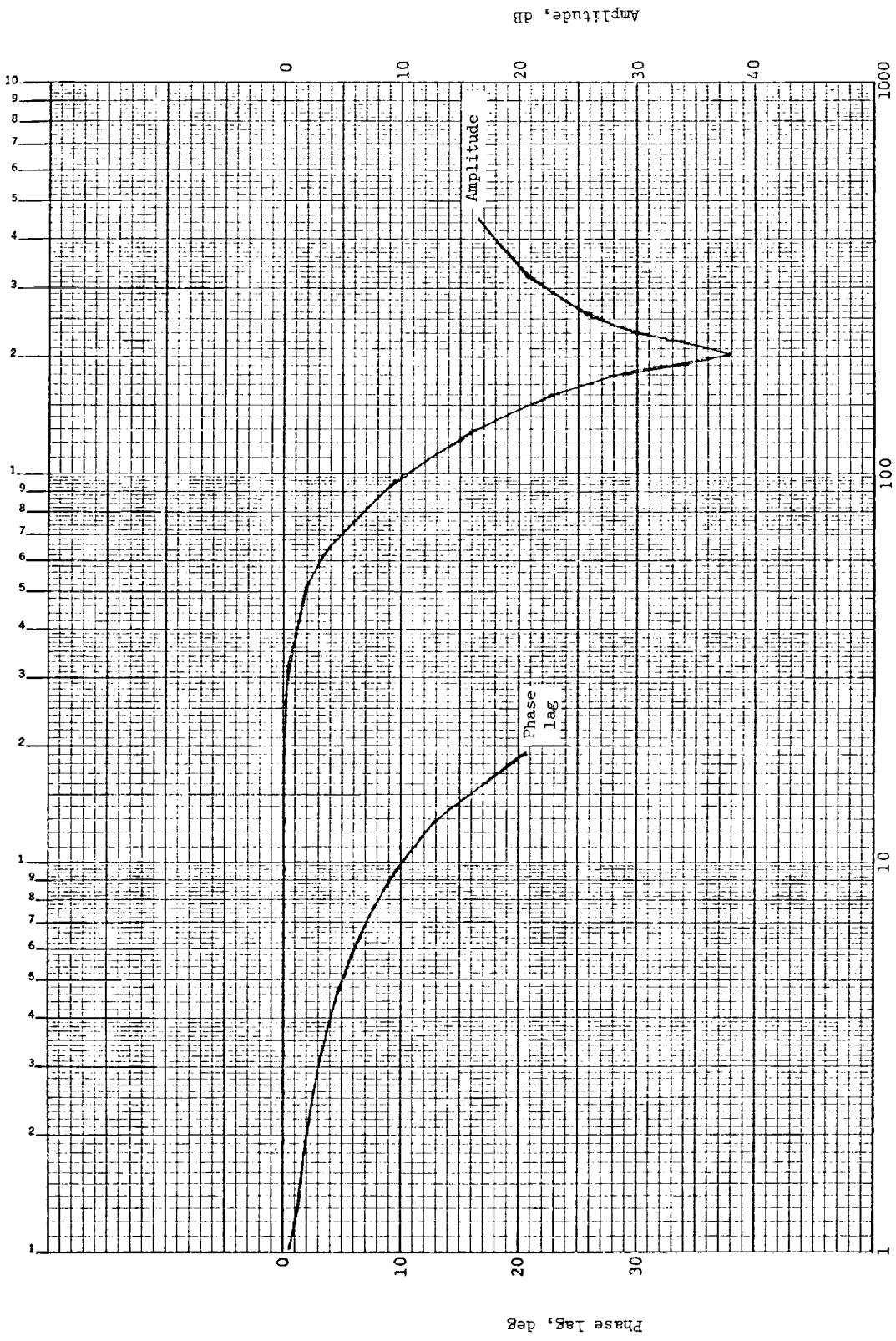

Figure 3.- Amplitude and phase characteristics of the notch filters.

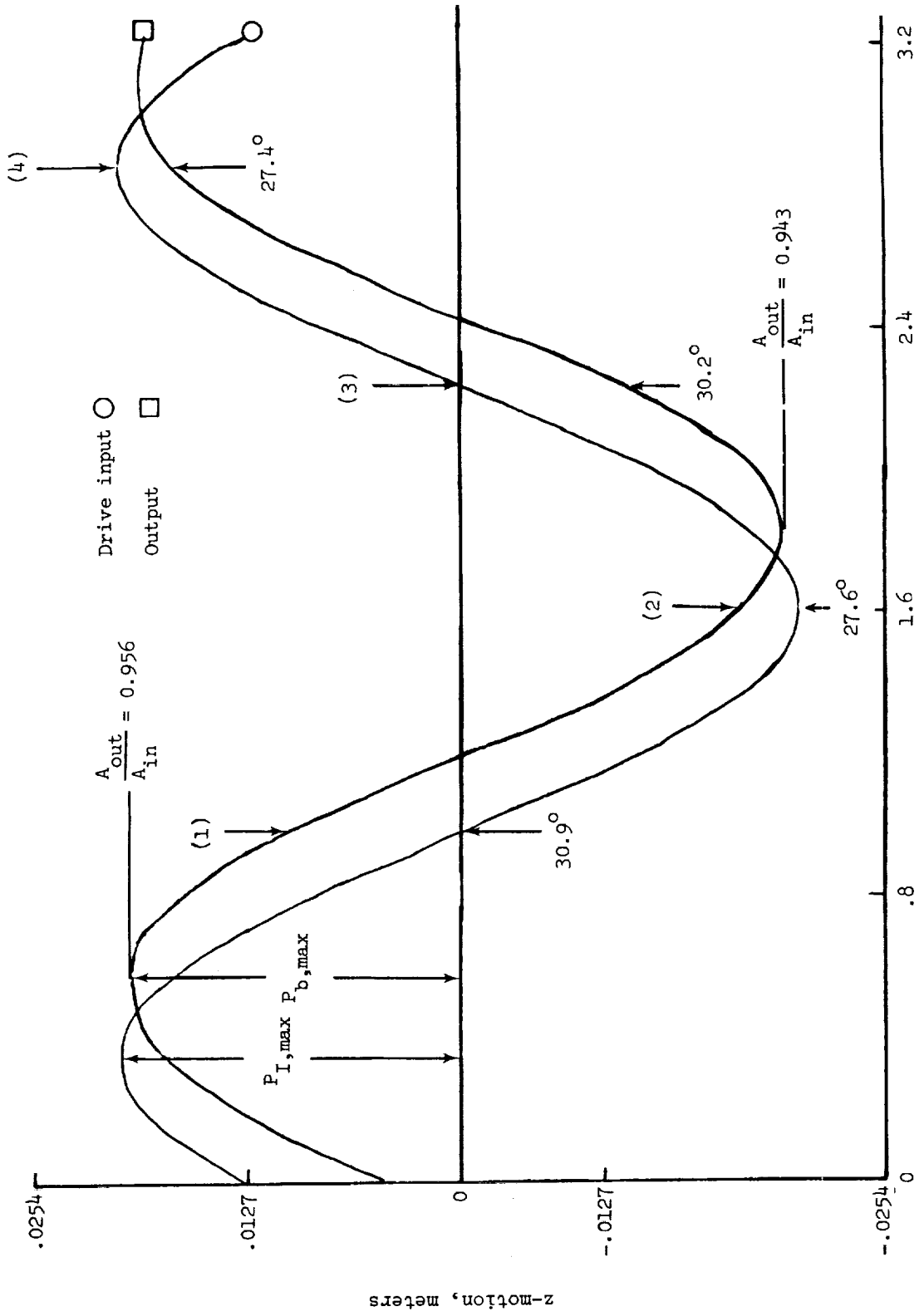

Figure 4.- Typical drive signal and base response. Frequency, 2.5 rad/sec; amplitude, 0.0203 meter.

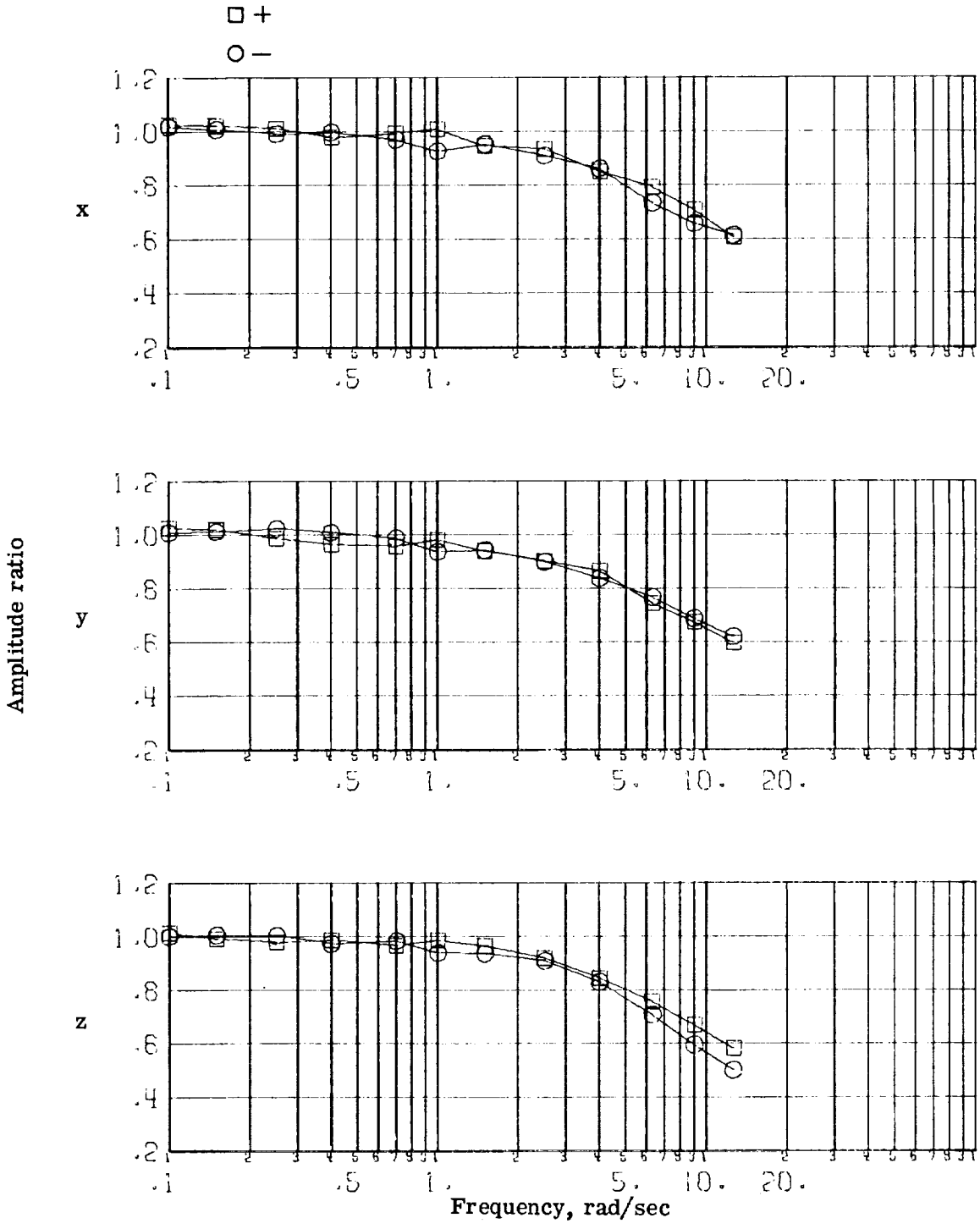

(a) Amplitude ratio.

Figure 5.- Translational channels for constant-amplitude input.

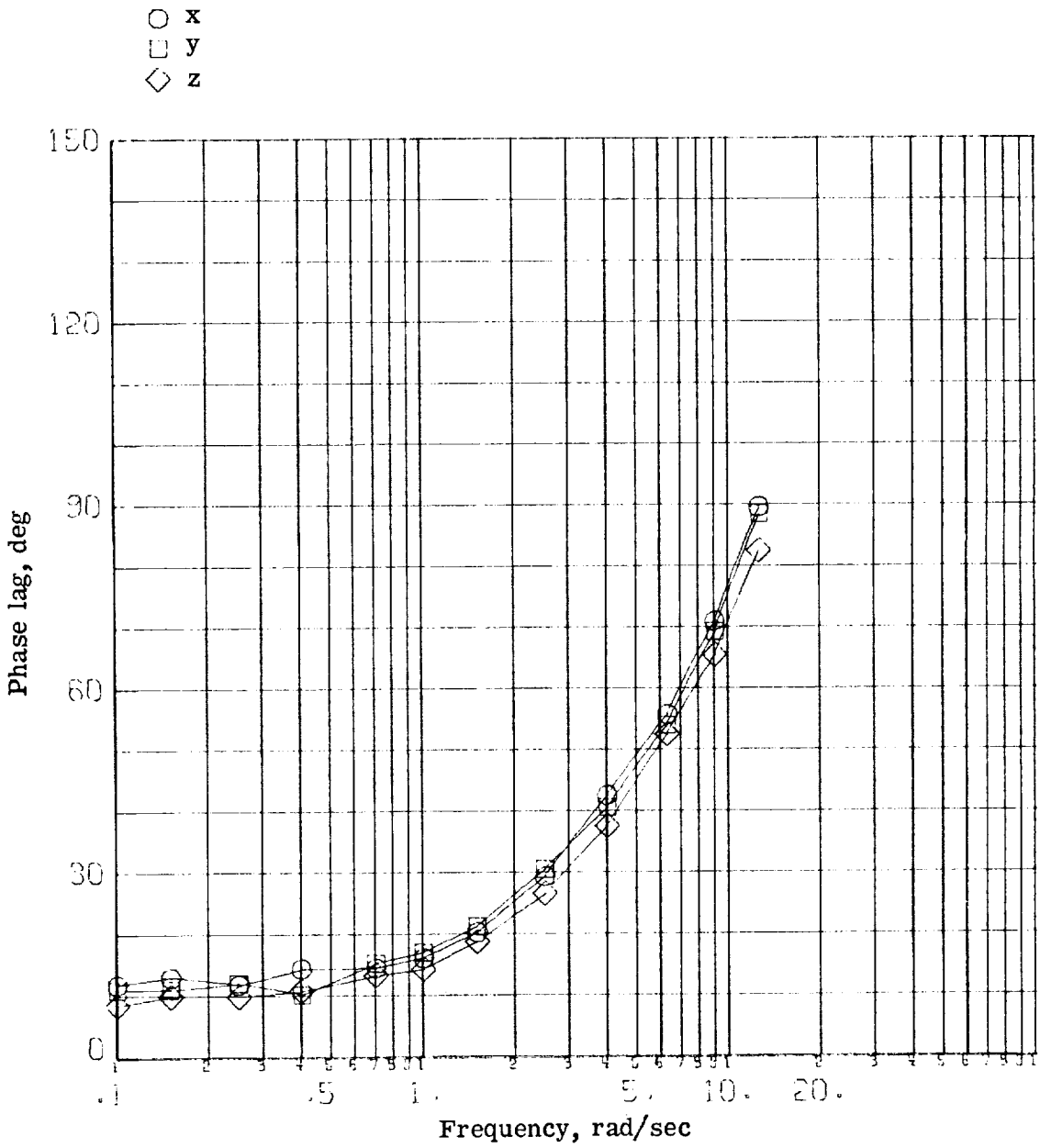

(b) Phase lag.

Figure 5.- Concluded.

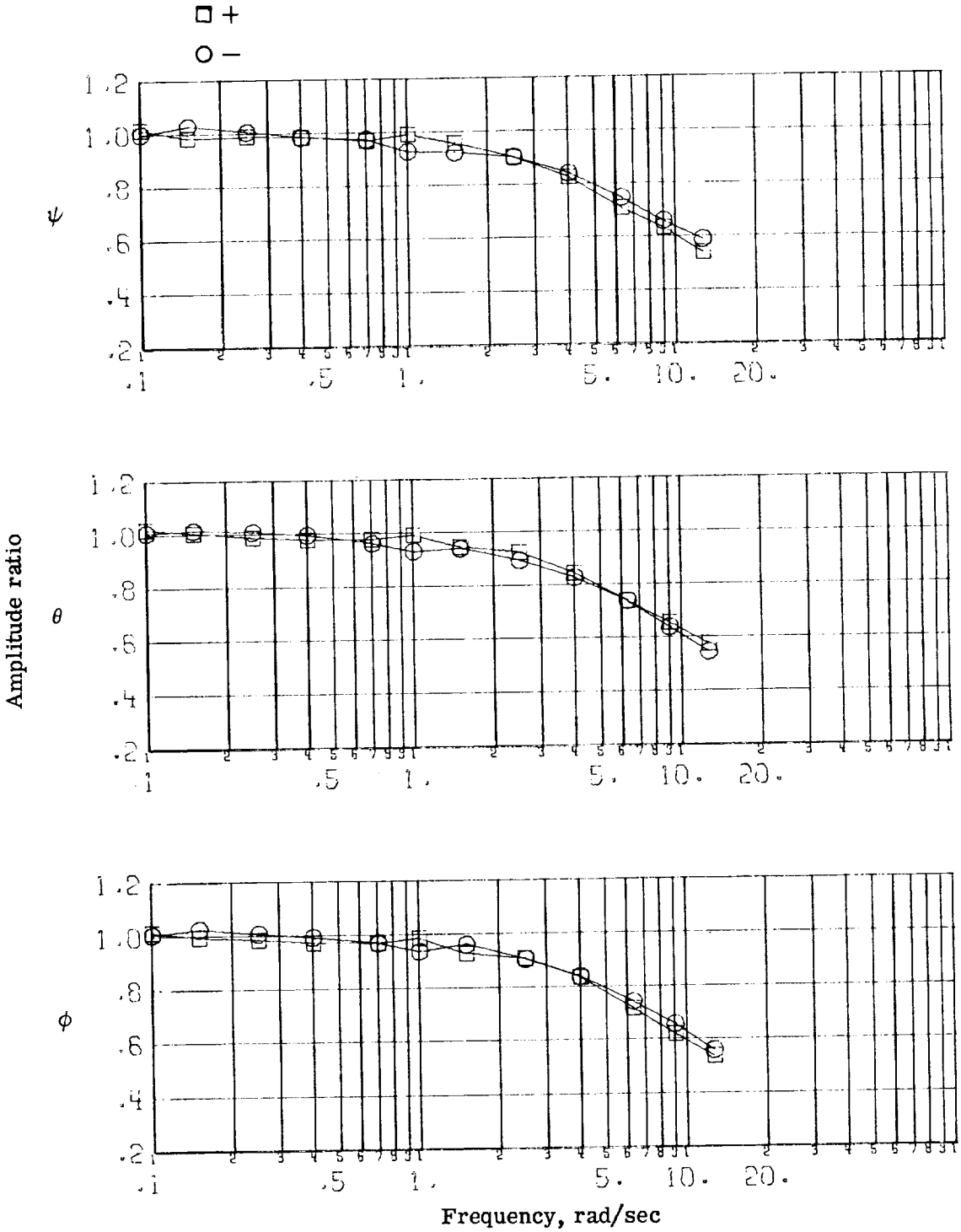

(a) Amplitude ratio.

Figure 6.- Rotational channels for constant-amplitude input.

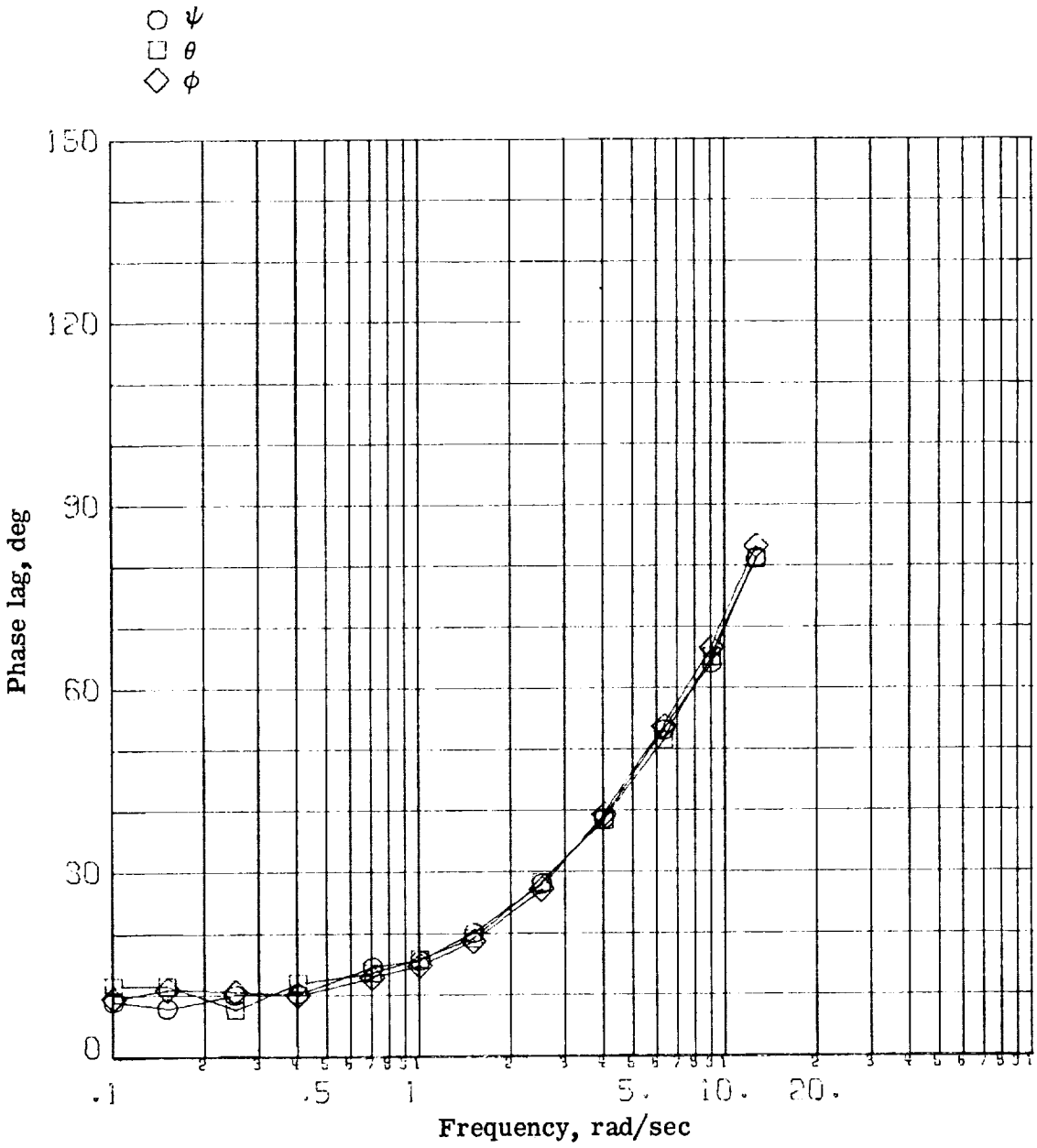

(b) Phase lag.

Figure 6.- Concluded.

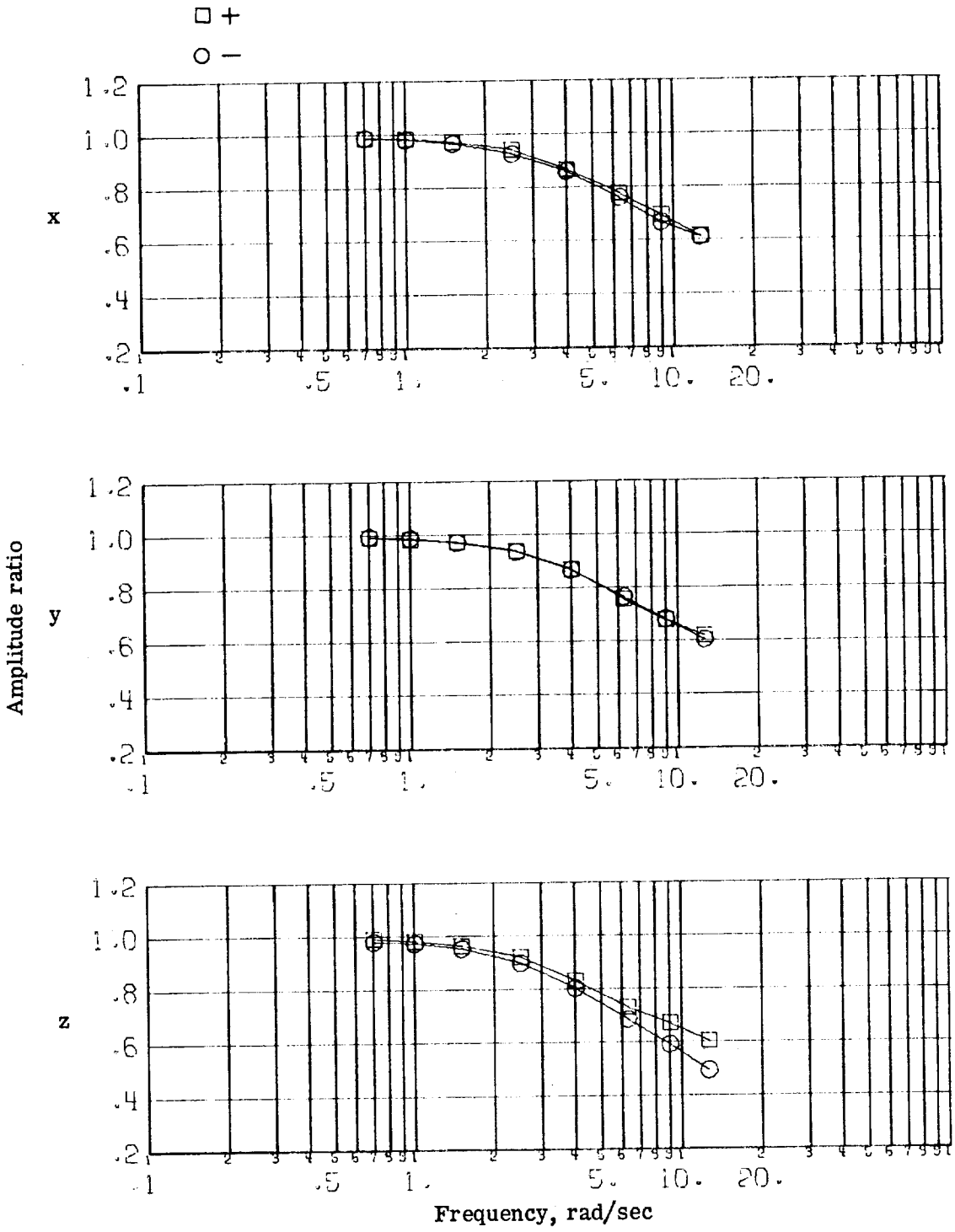

(a) Amplitude ratio for high-velocity case.

Figure 7.- Constant peak velocity response for translational channels.

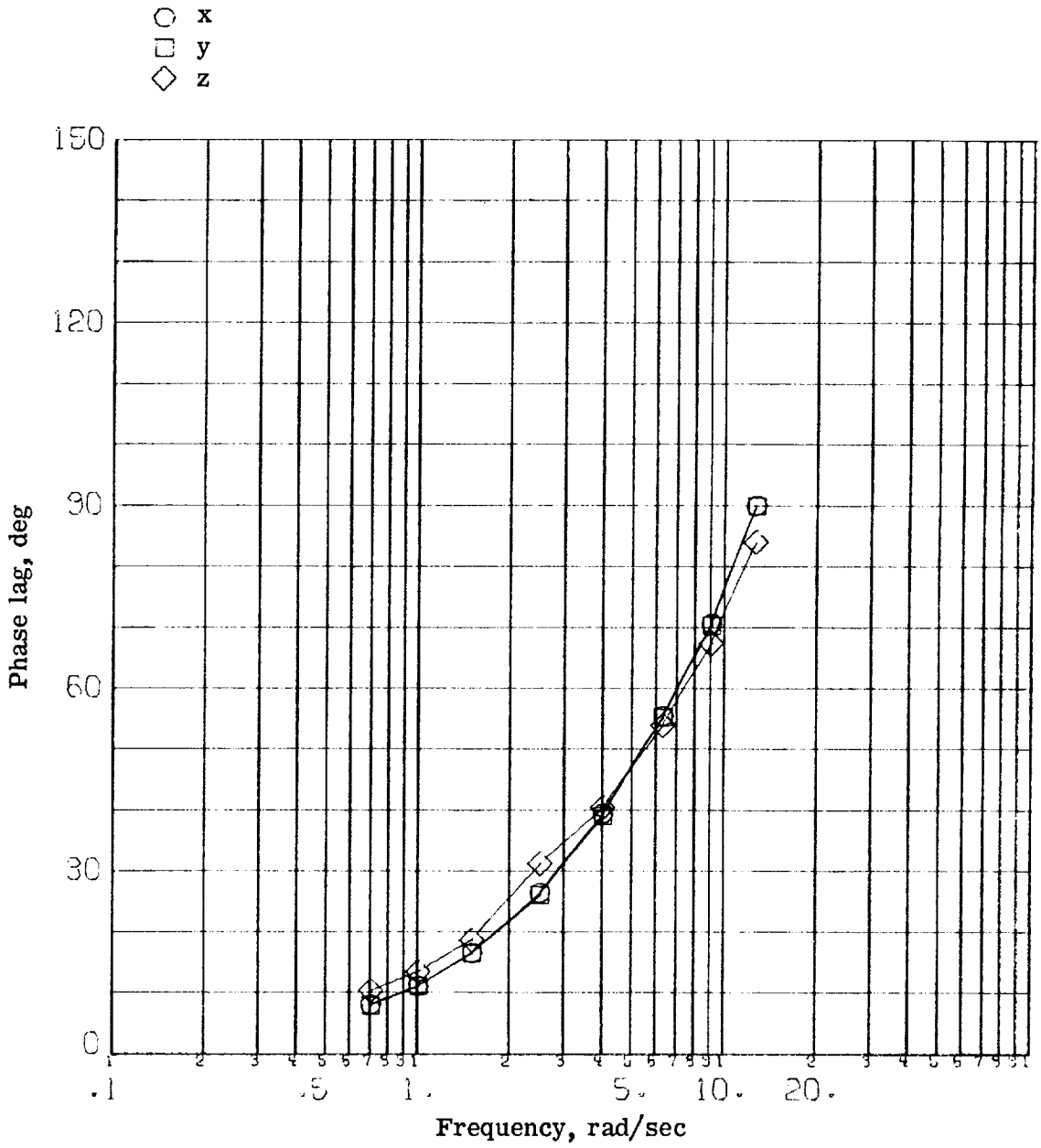

(b) Phase lag for high-velocity case.

Figure 7.- Continued.

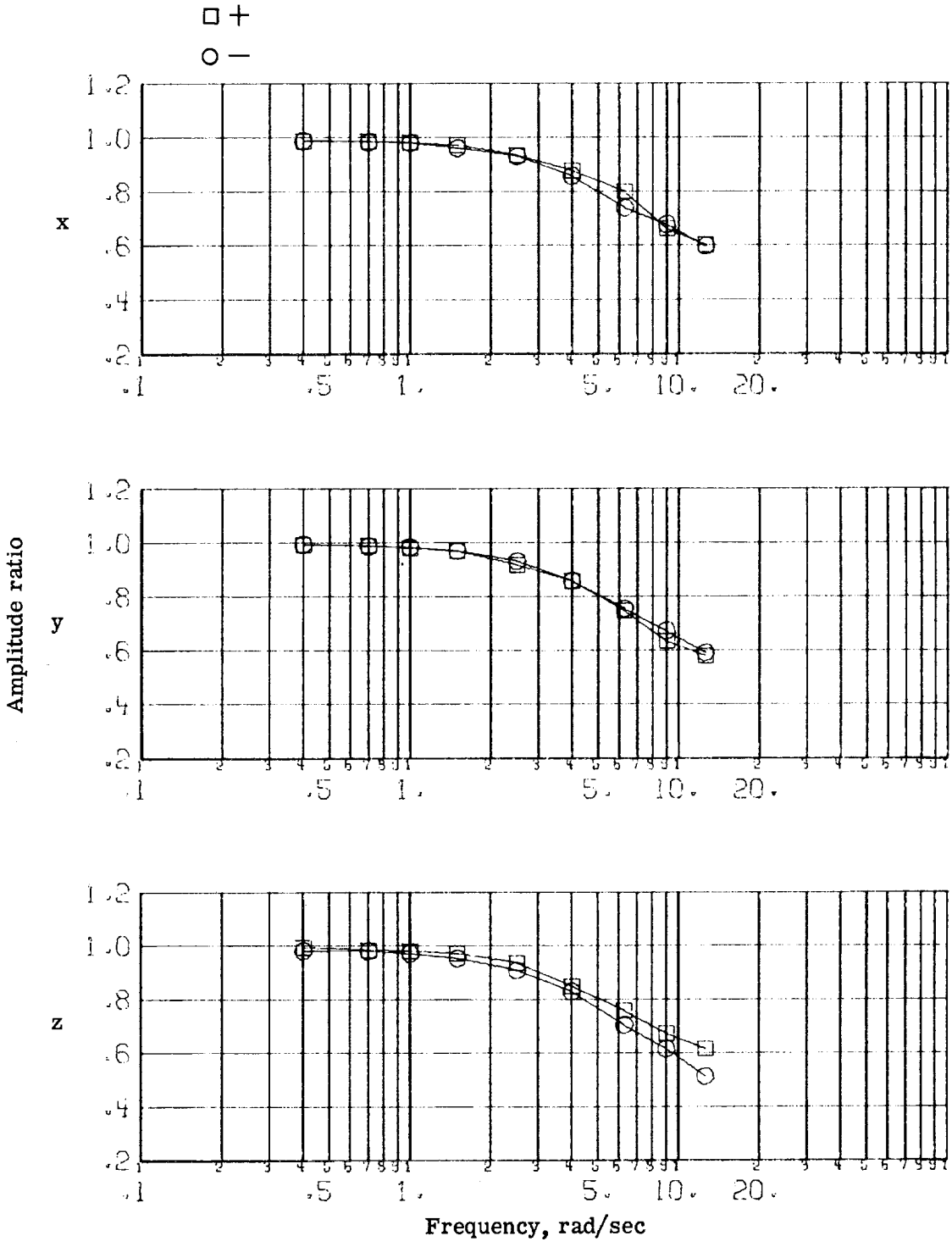

(c) Amplitude ratio for medium-velocity case.

Figure 7.- Continued.

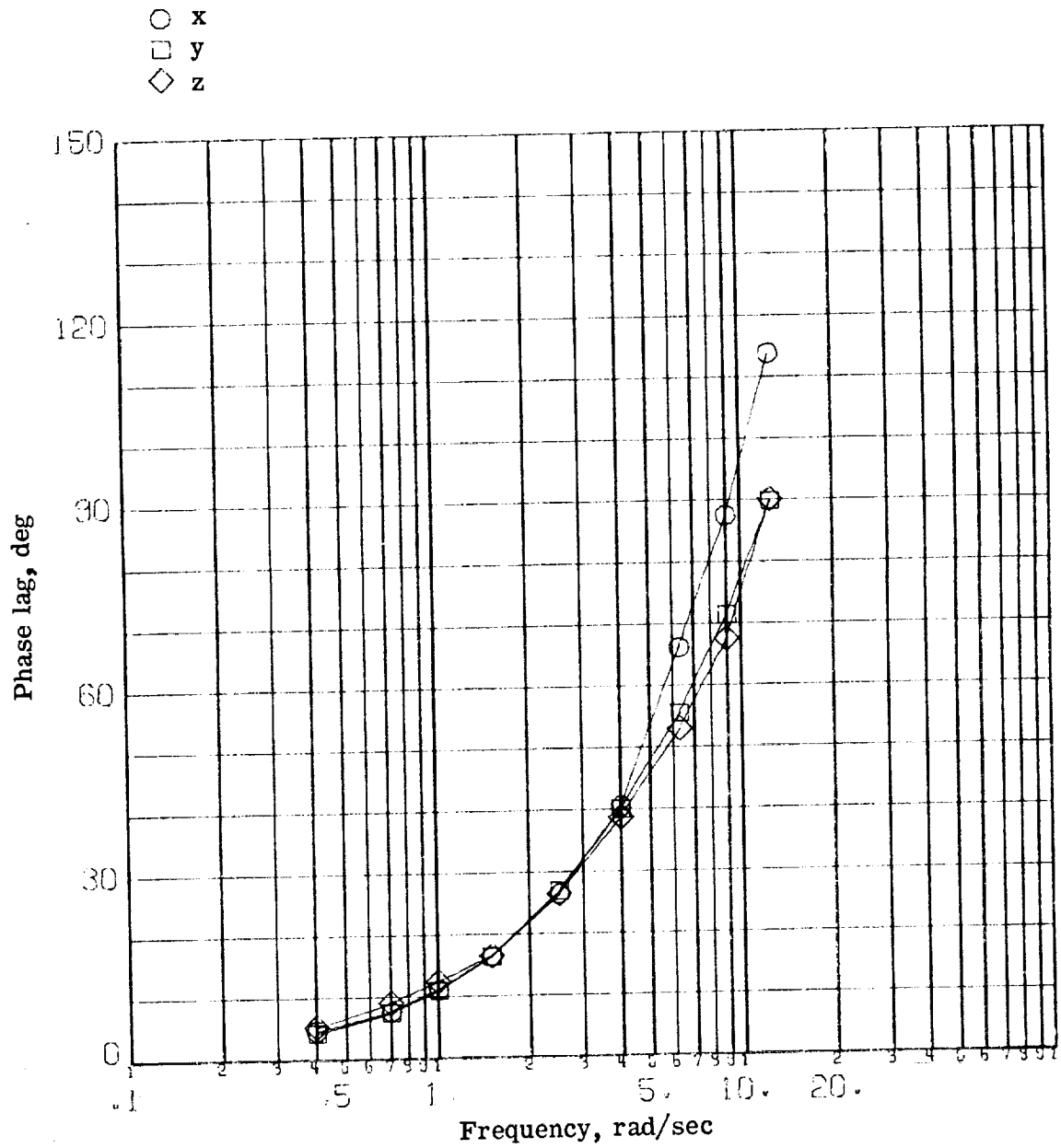

(d) Phase lag for medium-velocity case.

Figure 7.- Continued.

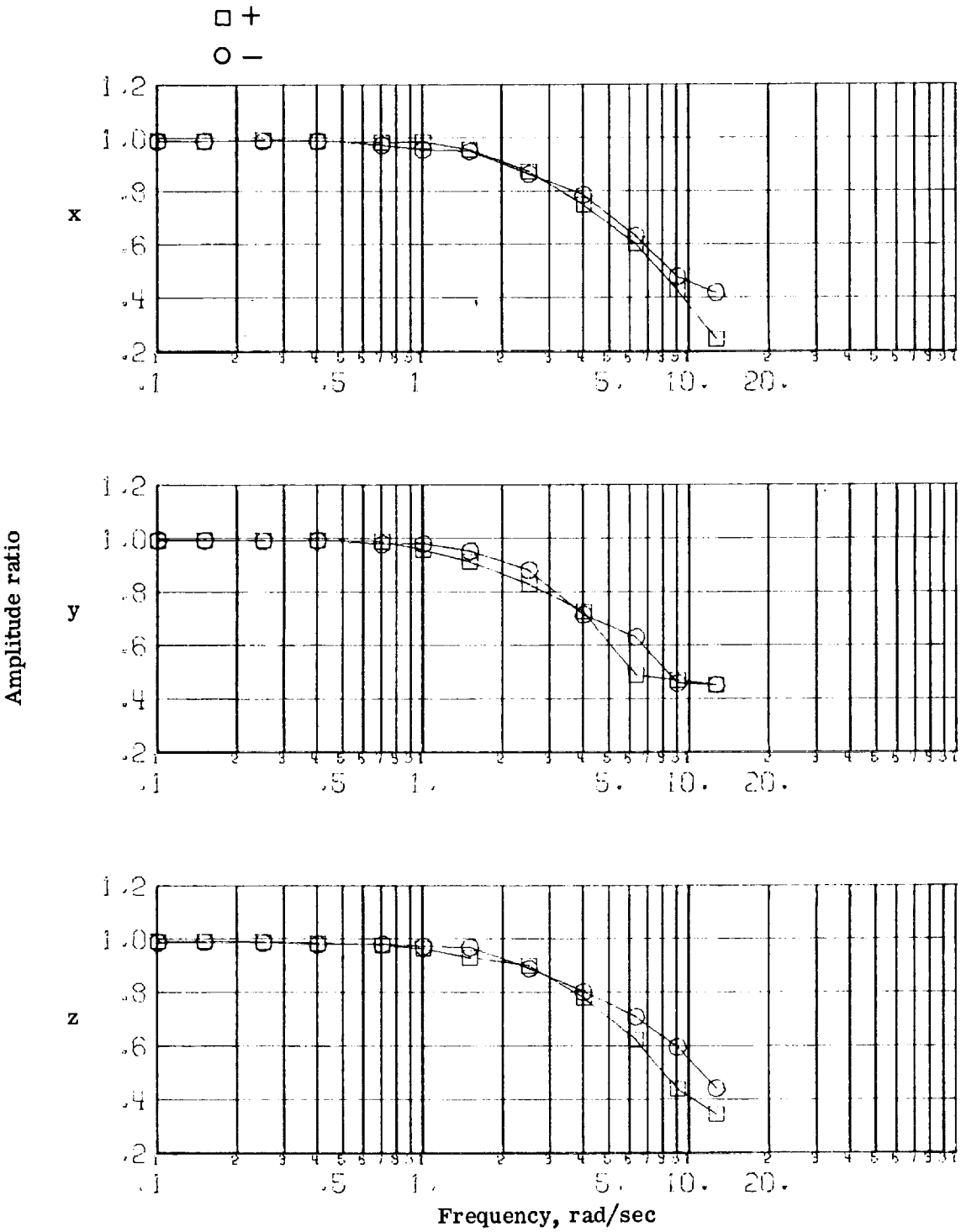

(e) Amplitude ratio for low-velocity case.

Figure 7.- Continued.

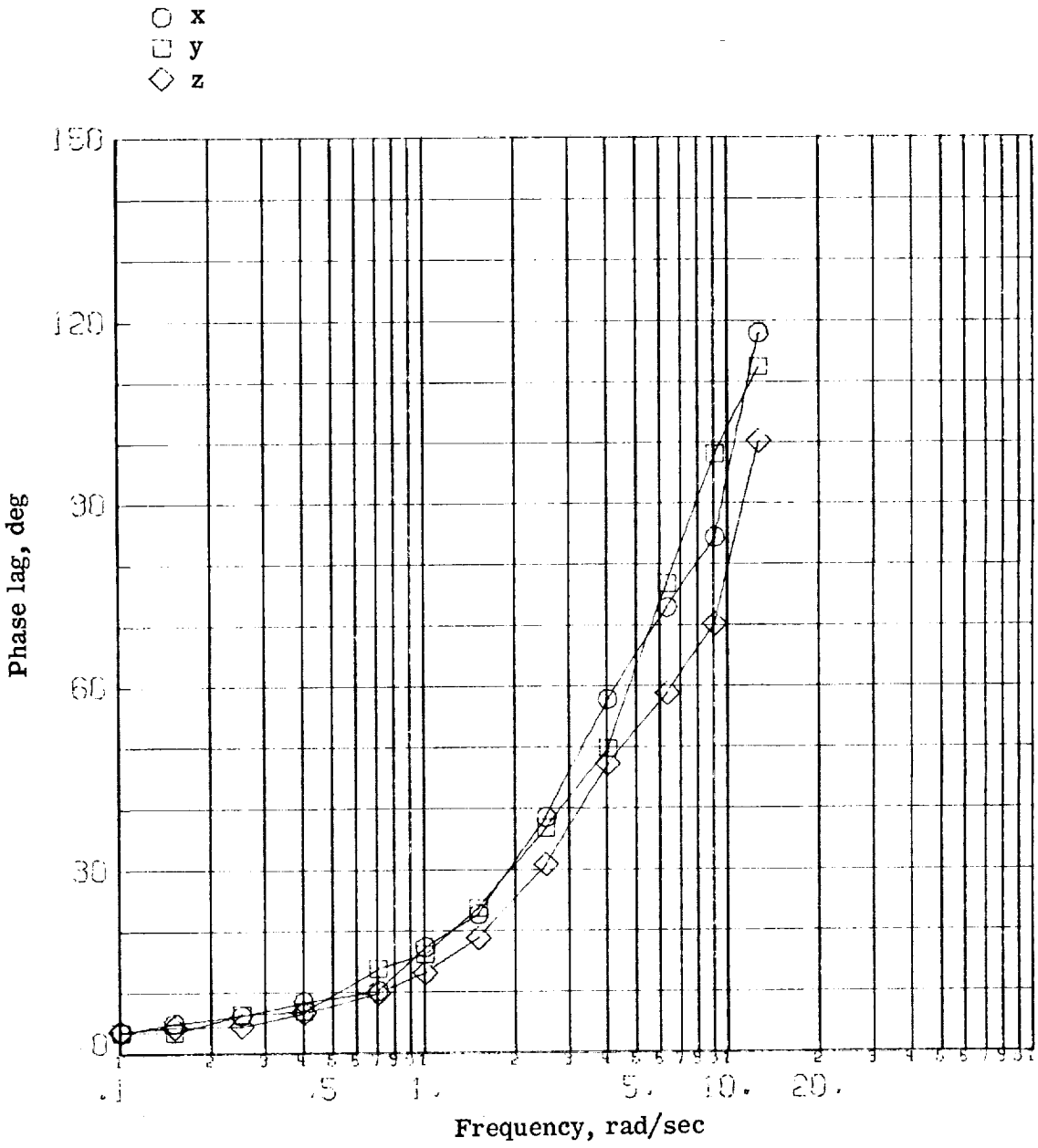

(f) Phase lag for low-velocity case.

Figure 7.- Concluded.

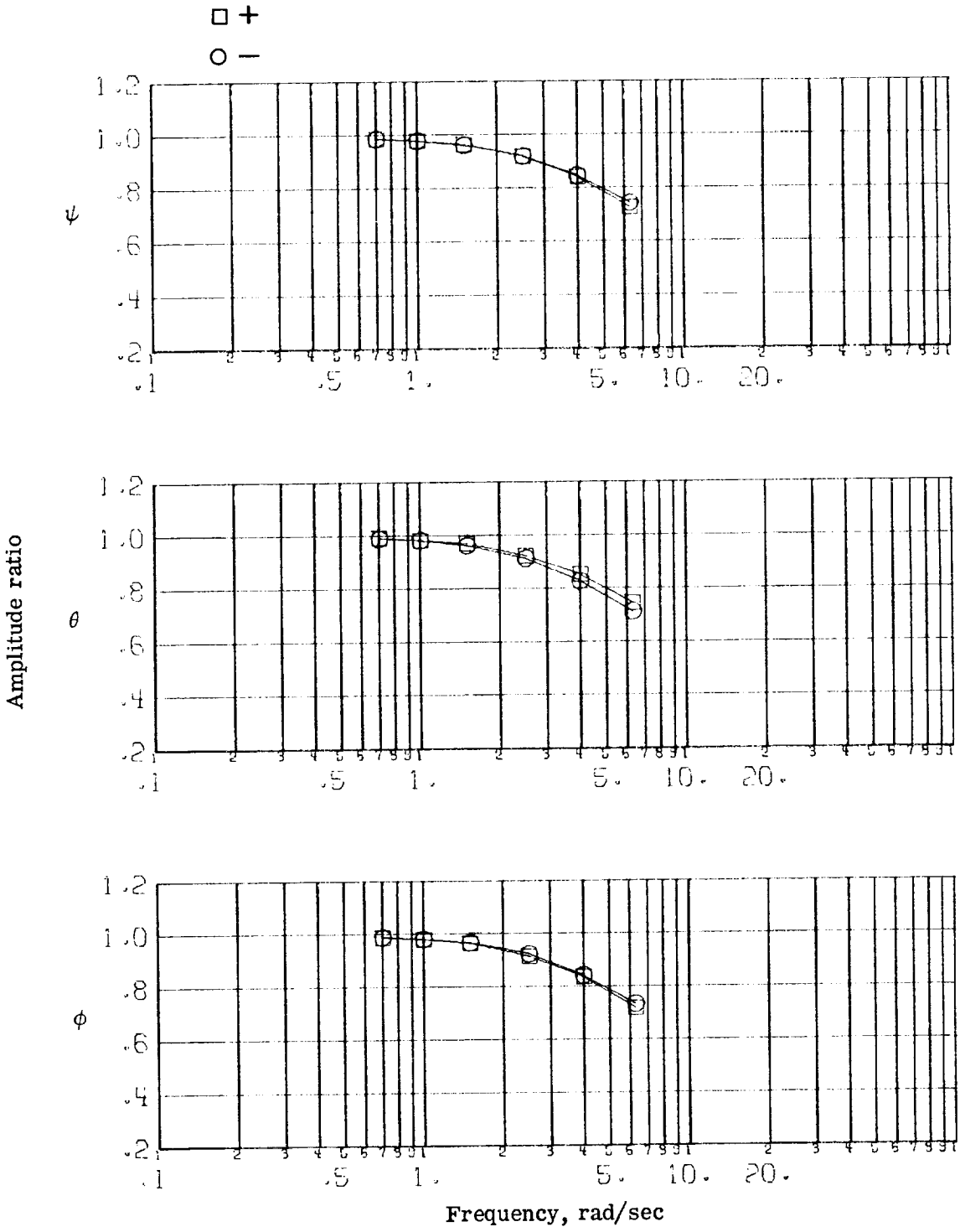

(a) Amplitude ratio for high-velocity case.

Figure 8.- Constant-peak-velocity response for rotational channels.

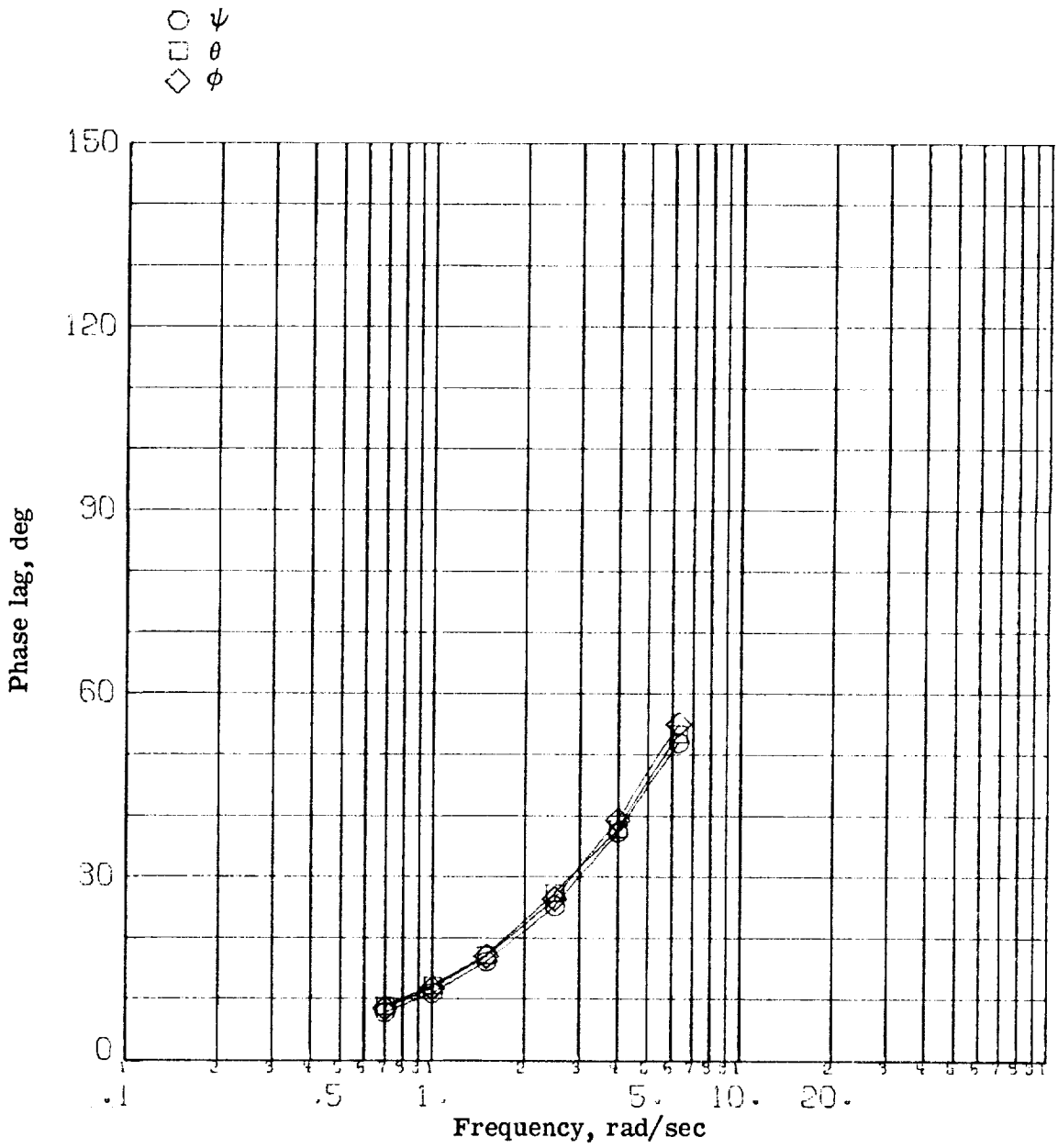

(b) Phase lag for high-velocity case.

Figure 8.- Continued.

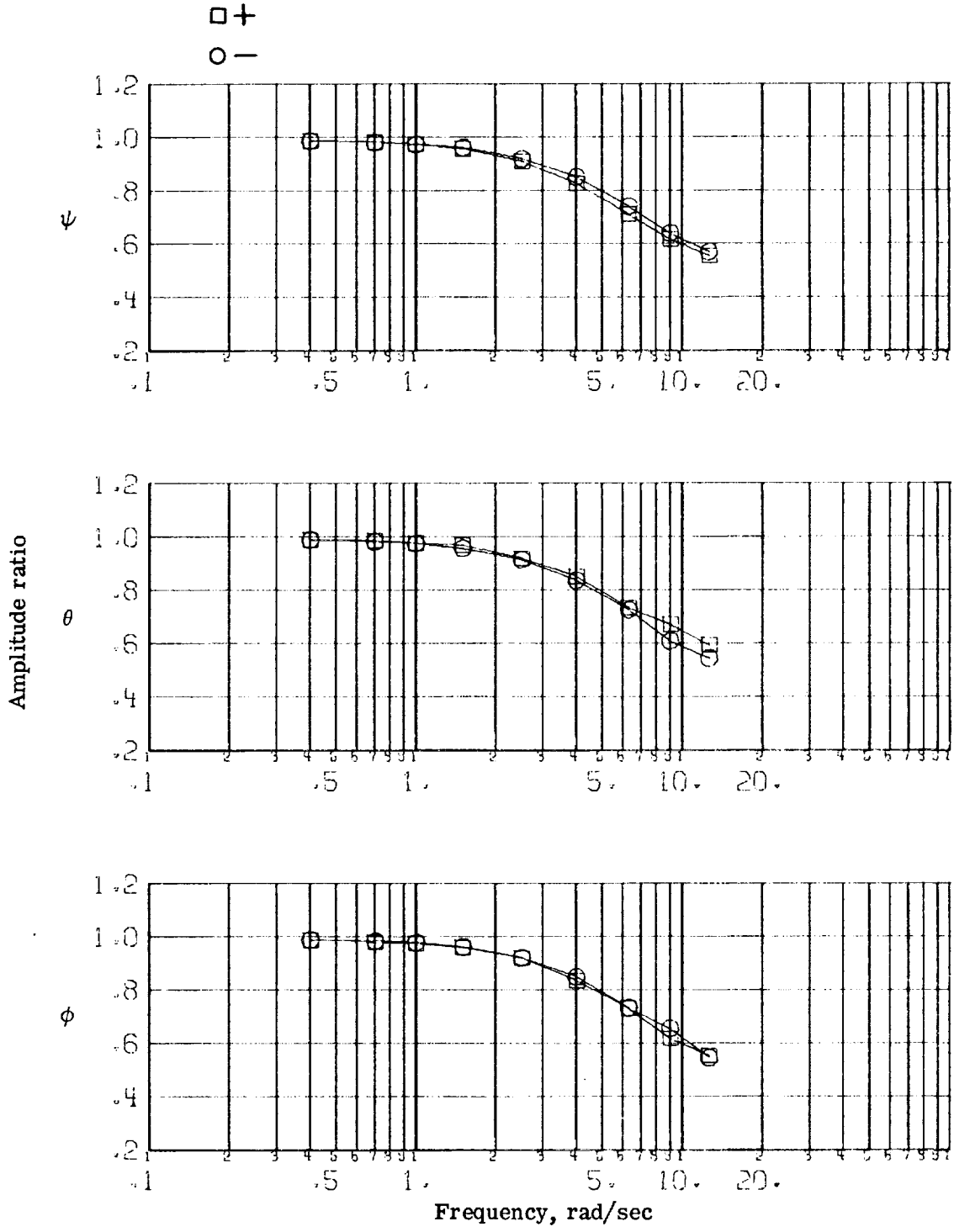

(c) Amplitude ratio for medium-velocity case.

Figure 8.- Continued.

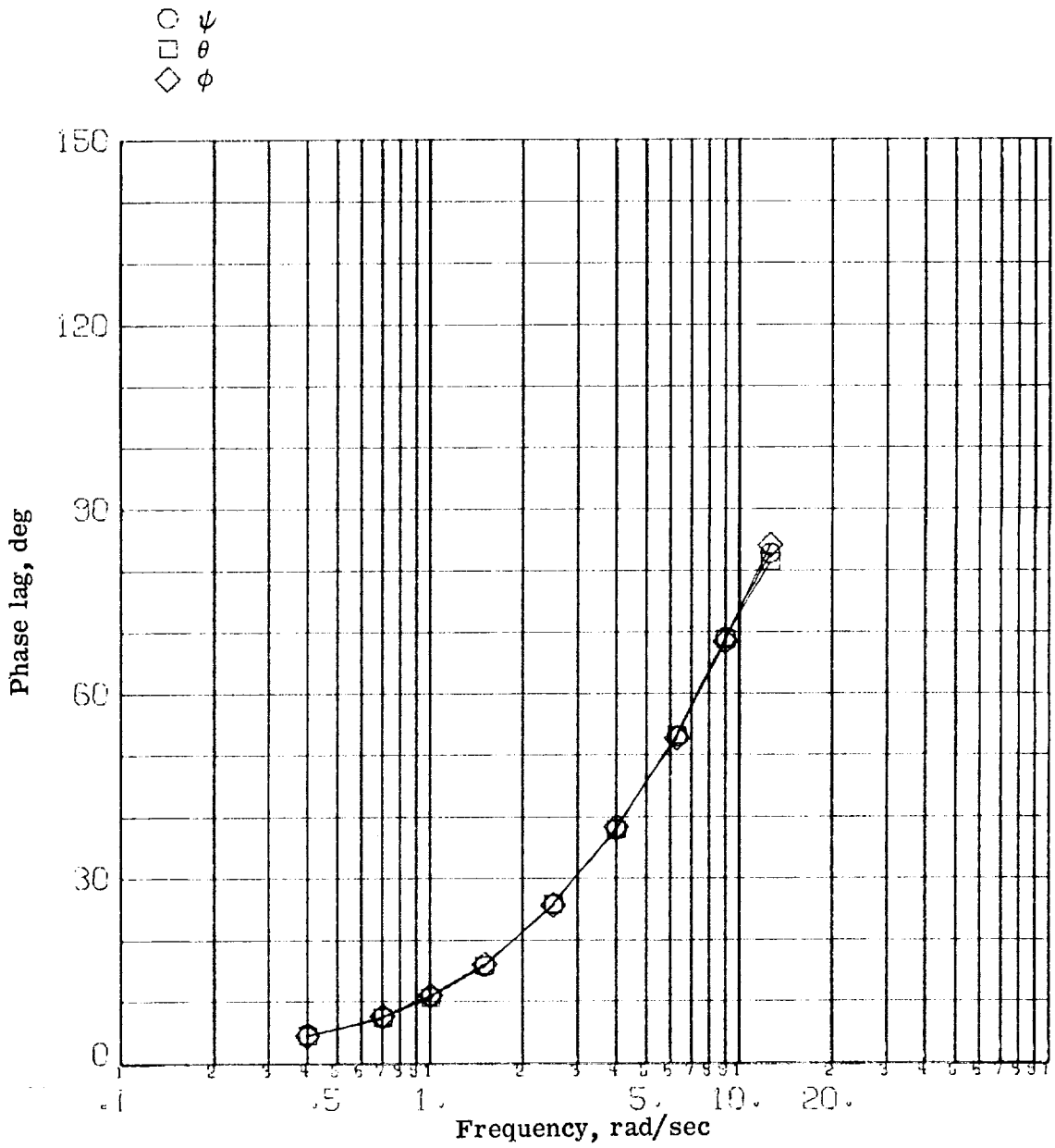

(d) Phase lag for medium-velocity case.

Figure 8.- Continued.

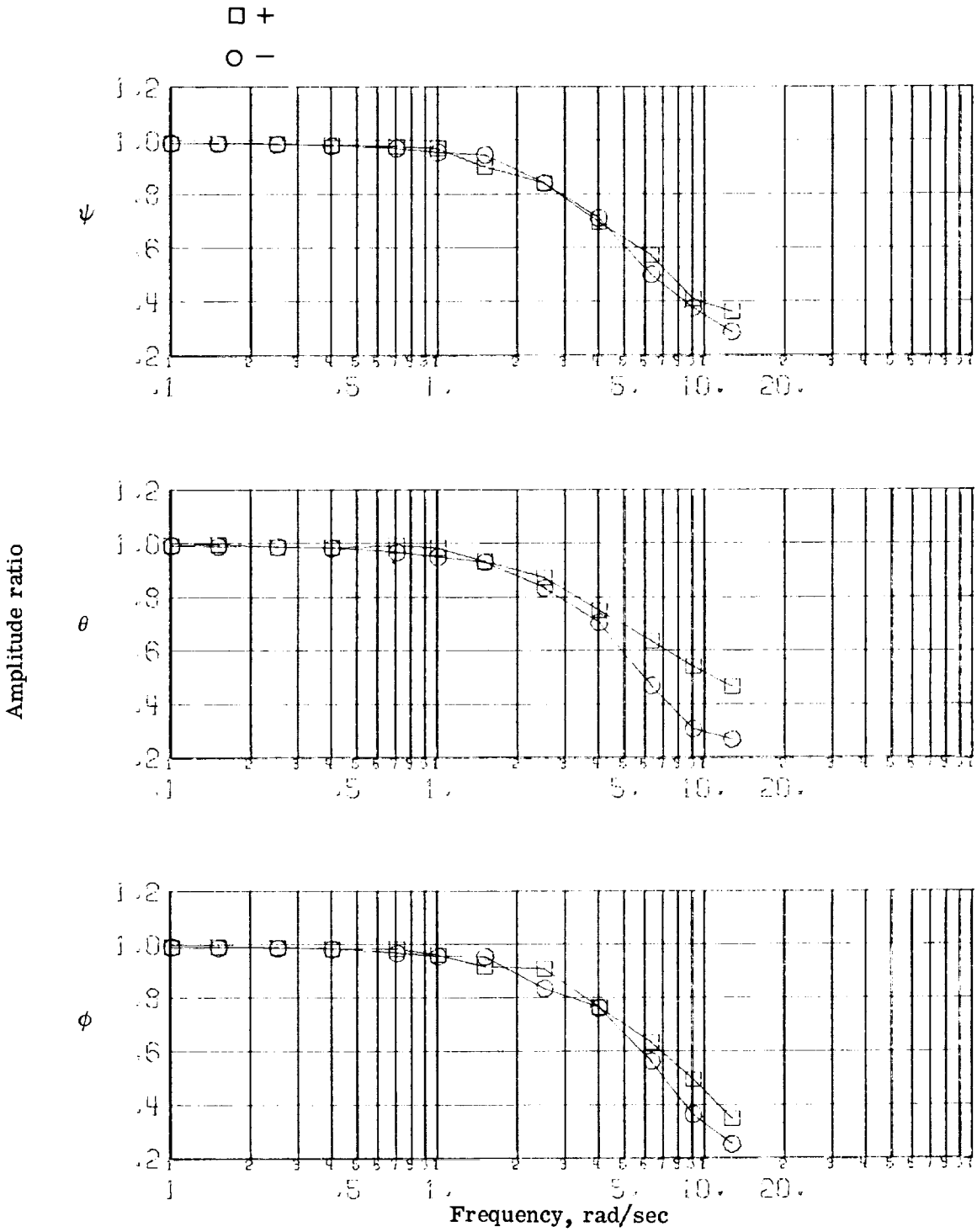

(e) Amplitude ratio for low-velocity case.

Figure 8.- Continued.

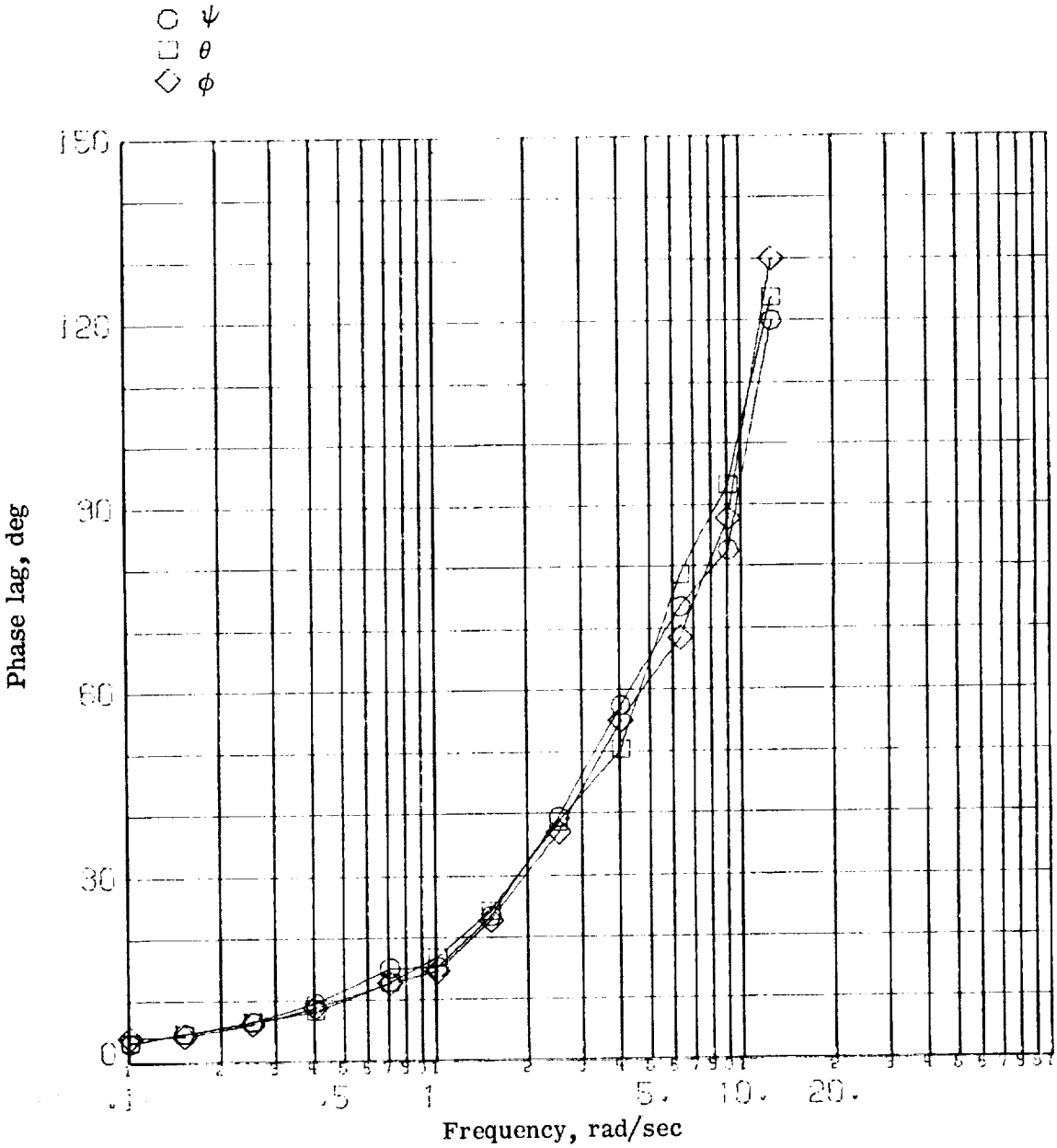

(f) Phase lag for low-velocity case.

Figure 8.- Concluded.

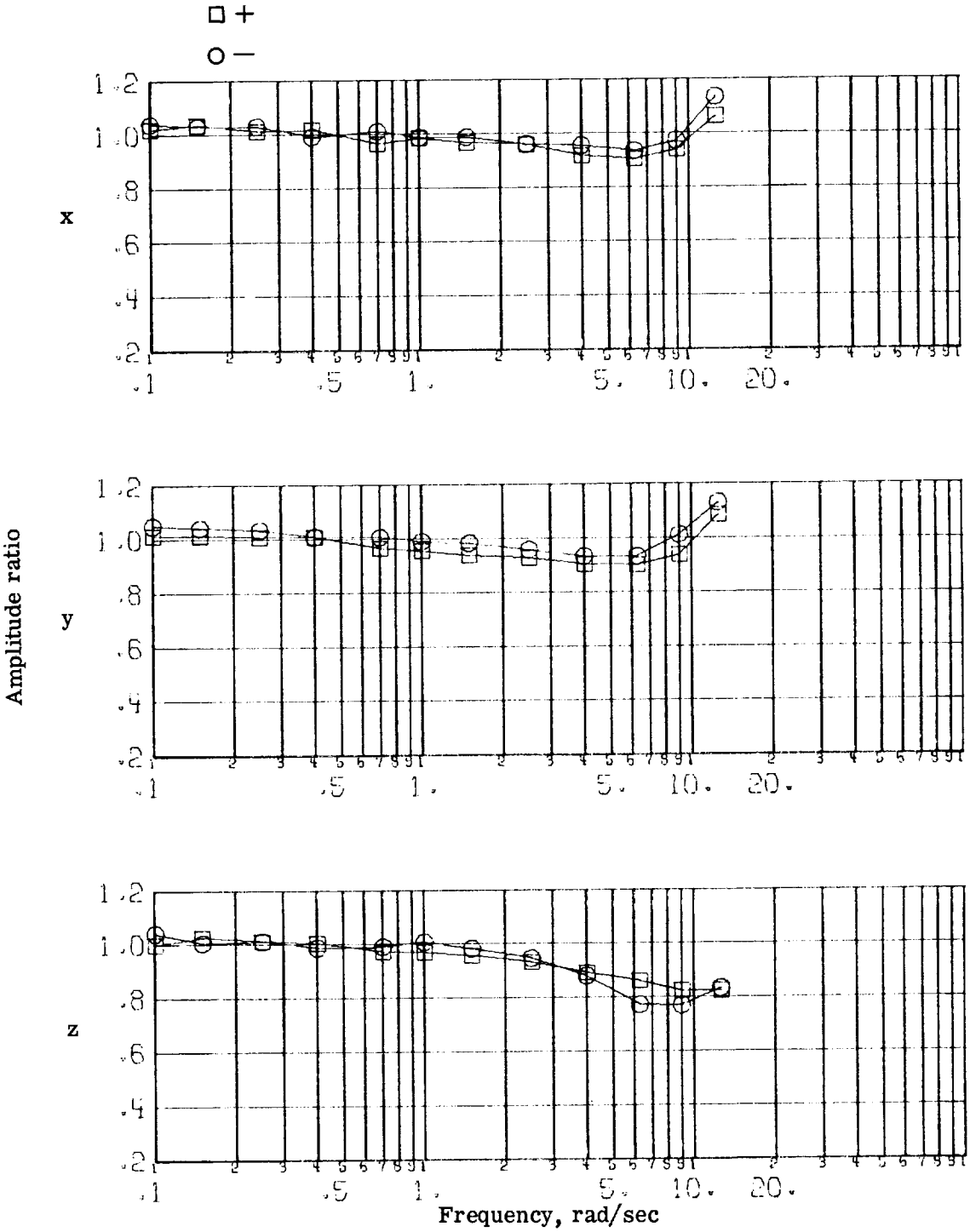

(a) Amplitude ratio.

Figure 9.- Compensated translational channels for constant-amplitude input.

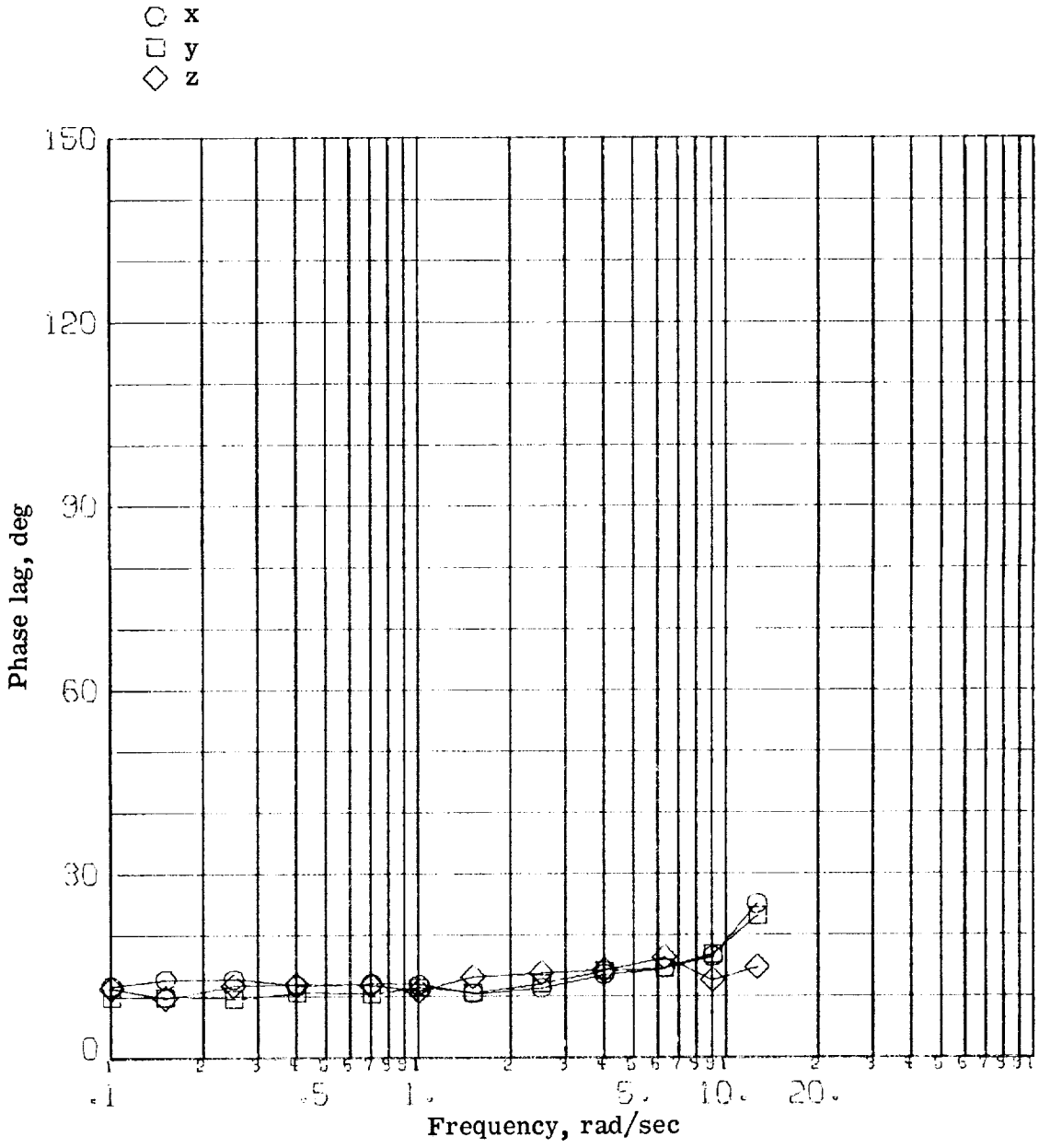

(b) Phase lag.

Figure 9.- Concluded.

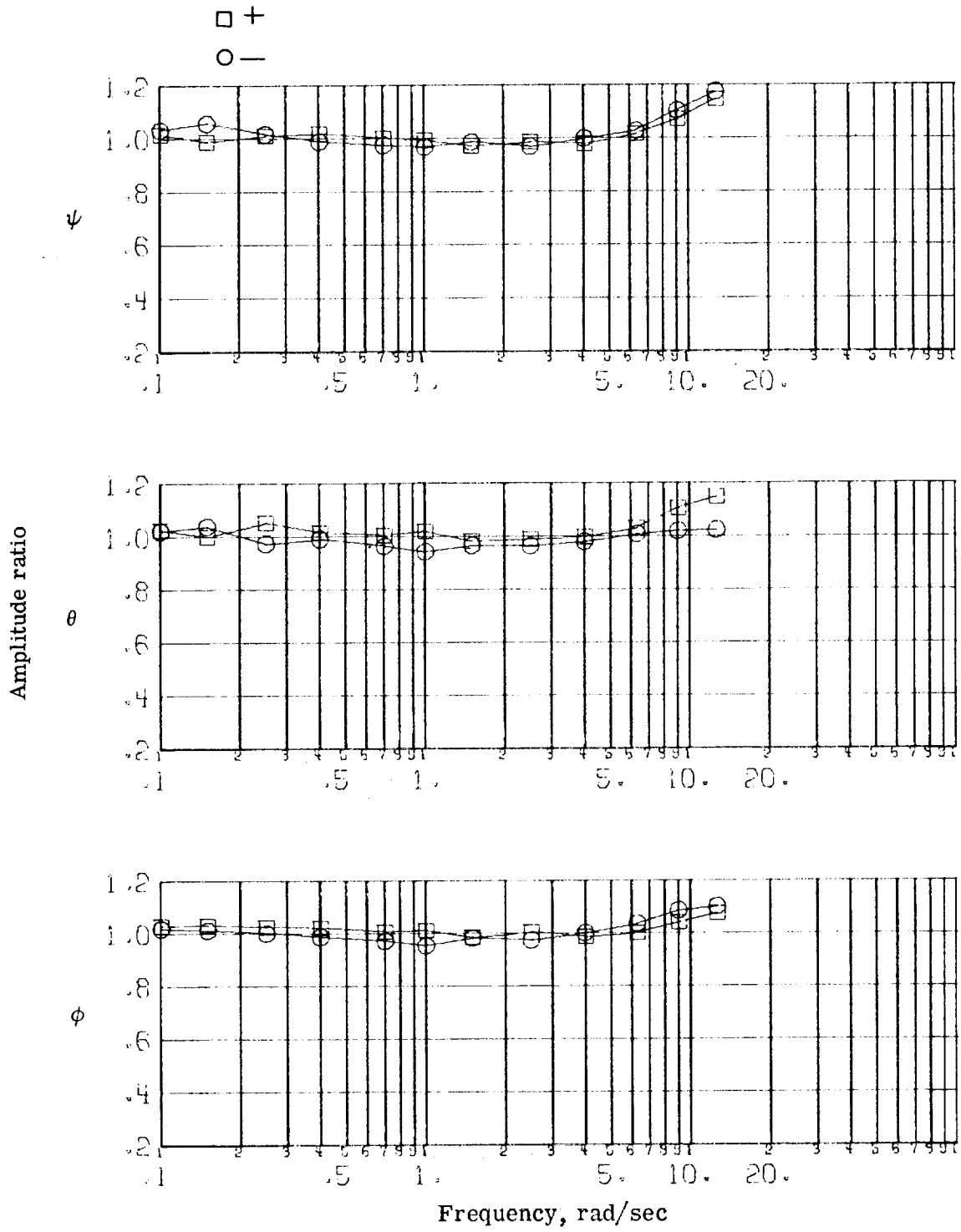

(a) Amplitude ratio.

Figure 10.- Compensated rotational channels for constant-amplitude input.

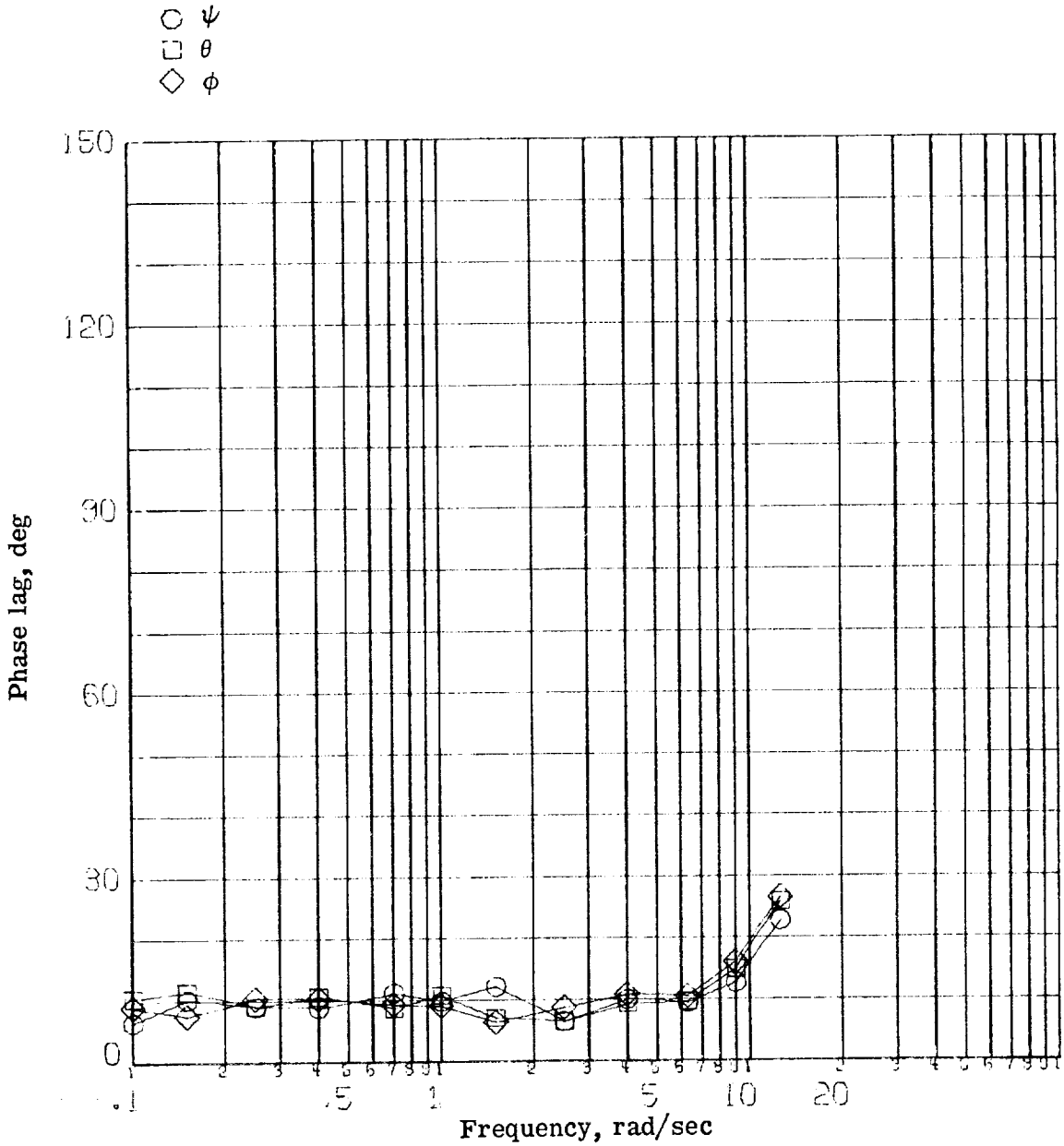

(b) Phase lag.

Figure 10.- Concluded.

NASA-Langley, 1973 —— 11 L-9023